...ED STATES
...MENT OF
...MERCE
PUBLICATION

NOAA Technical Memorandum NWS TDL-50

U.S. DEPARTMENT OF COMMERCE
National Oceanic and Atmospheric Administration
National Weather Service

Forecasting Extratropical Storm Surges For the Northeast Coast of the United States

N. ARTHUR PORE
WILLIAM S. RICHARDSON
HERMAN P. PERROTTI

WASHINGTON, D.C.
...nuary 1974

NOAA TECHNICAL MEMORANDA

National Weather Service, Techniques Development Laboratory Series

The primary purpose of the Techniques Development Laboratory of the Office of Systems Development is to translate increases of basic knowledge in meteorology and allied disciplines into improved operating techniques and procedures. To achieve this goal, the laboratory conducts applied research and development aimed at the improvement of diagnostic and prognostic methods for producing weather information. The laboratory performs studies both for the general improvement of prediction methodology used in the National Meteorological Service and for the more effective utilization of weather forecasts by the ultimate user.

NOAA Technical Memoranda in the National Weather Service Techniques Development Laboratory series facilitate rapid distribution of material that may be preliminary in nature and which may be published formally elsewhere at a later date. Publications 1 through 5 are in the former series, Weather Bureau Technical Notes (TN), Techniques Development Laboratory (TDL) Reports; publications 6 through 36 are in the former series, ESSA Technical Memoranda, Weather Bureau Technical Memoranda (WBTM). Beginning with TDL 37, publications are now part of the series NOAA Technical Memoranda, National Weather Service (NWS).

Publications listed below are available from the National Technical Information Service (NTIS), U.S. Department of Commerce, Sills Bldg., 5285 Port Royal Road, Springfield, Va. 22151. Prices vary for paper copy; $1.45 microfiche. Order by accession number, when given, in parentheses at end of each entry.

Weather Bureau Technical Notes

TN 10 TDL 1 Objective Prediction of Daily Surface Temperature. William H. Klein, Curtis W. Crockett, and Carlos R. Dunn, October 1965. (PB-168-590)

TN 11 TDL 2 Hurricane Cindy Galveston Bay Tides. N. A. Pore, A. T. Angelo, and J. G. Taylor, September 1965. (PB-168-608)

TN 29 TDL 3 Atmospheric Effects on Re-Entry Vehicle Dispersions. Karl R. Johannessen, December 1965. (PB-169-381)

TN 45 TDL 4 A Synoptic Climatology of Winter Precipitation from 700-mb. Lows for the Intermountain Areas of the West. Donald L. Jorgensen, William H. Klein, and August F. Korte, May 1966. (PB-170-635)

TN 47 TDL 5 Hemispheric Specification of Sea Level Pressure from Numerical 700-mb. Height Forecasts. William H. Klein and Billy M. Lewis, June 1966. (PB-173-091)

ESSA Technical Memoranda

WBTM TDL 6 A Fortran Program for the Calculation of Hourly Values of Astronomical Tide and Time and Height of High and Low Water. N. A. Pore and R. A. Cummings, January 1967. (PB-174-660)

WBTM TDL 7 Numerical Experiments Leading to the Design of Optimum Global Meteorological Networks. M. A. Alaka and F. Lewis, February 1967. (PB-174-497)

WBTM TDL 8 An Experiment in the Use of the Balance Equation in the Tropics. M. A. Alaka, D. T. Rubsam, and G. E. Fisher, March 1967. (PB-174-501)

WBTM TDL 9 A Survey of Studies of Aerological Network Requirements. M. A. Alaka, May 1967. (PB-174-984)

WBTM TDL 10 Objective Determination of Sea Level Pressure from Upper Level Heights. William Klein, Frank Lewis, and John Stackpole, May 1967. (PB-179-949)

WBTM TDL 11 Short Range, Subsynoptic Surface Weather Prediction. H. R. Glahn and D. A. Lowry, July 1967. (PB-175-772)

WBTM TDL 12 Charts Giving Station Precipitation in the Plateau States From 700-Mb. Lows During Winter. Donald L. Jorgensen, August F. Korte, and James A. Bunce, Jr., October 1967. (PB-176-742)

WBTM TDL 13 Interim Report on Sea and Swell Forecasting. N. A. Pore and W. S. Richardson, December 1967. (PB-177-038)

WBTM TDL 14 Meteorological Analysis of 1964-65 ICAO Turbulence Data. DeVer Colson, October 1968. (PB-180-268)

WBTM TDL 15 Prediction of Temperature and Dew Point by Three-Dimensional Trajectories. Ronald M. Reap, October 1968. (PB-180-727)

WBTM TDL 16 Objective Visibility Forecasting Techniques Based on Surface and Tower Observations. Donald M. Gales, October 1968. (PB-180-479)

WBTM TDL 17 Second Interim Report on Sea and Swell Forecasting. N. A. Pore and W. S. Richardson, January 1969. (PB-182-273)

WBTM TDL 18 Conditional Probabilities of Precipitation Amounts in the Conterminous United States. Donald L. Jorgensen, William H. Klein, and Charles F. Roberts, March 1969. (PB-183-144)

WBTM TDL 19 An Operationally Oriented Small-Scale 500-Millibar Height Analysis Program. Harry R. Glahn and George W. Hollenbaugh, March 1969. (PB-184-111)

WBTM TDL 20 A Comparison of Two Methods of Reducing Truncation Error. Robert J. Bermowitz, May 1969. (PB-184-741)

WBTM TDL 21 Automatic Decoding of Hourly Weather Reports. George W. Hollenbaugh, Harry R. Glahn, and Dale A. Lowry, July 1969. (PB-185-806)

WBTM TDL 22 An Operationally Oriented Objective Analysis Program. Harry R. Glahn, George W. Hollenbaugh, and Dale A. Lowry, July 1969. (PB-186-129)

WBTM TDL 23 An Operational Subsynoptic Advection Model. Harry R. Glahn, Dale A. Lowry, and George W. Hollenbaugh, July 1969. (PB-186-389)

WBTM TDL 24 A Lake Erie Storm Surge Forecasting Technique. William S. Richardson and N. Arthur Pore, August 1969. (PB-185-778)

(Continued on inside back cover)

U.S. DEPARTMENT OF COMMERCE
National Oceanic and Atmospheric Administration
National Weather Service

NOAA Technical Memorandum NWS TDL-50

FORECASTING EXTRATROPICAL STORM SURGES FOR THE NORTHEAST COAST OF THE UNITED STATES

N. Arthur Pore, William S. Richardson,
and Herman P. Perrotti

Systems Development Office
Techniques Development Laboratory

SILVER SPRING, MD.

January 1974

CONTENTS

FORECASTING EXTRATROPICAL STORM SURGES FOR THE NORTHEAST COAST OF THE UNITED STATES

N. Arthur Pore, William S. Richardson, and Herman P. Perrotti
Techniques Development Laboratory
Systems Development Office, NOAA, Silver Spring, Md.

ABSTRACT. The National Weather Service (NWS) has developed a technique for forecasting extratropical storm surges along the northeast coast of the United States. The storm surge is caused mainly by the strong winds associated with extratropical storms over nearshore areas.

Empirical forecast equations have been derived for 10 locations from Portland, Maine to Norfolk, Va. with data from 68 storms that occurred from 1956 through 1969. Input data to the technique are sea-level pressure values as forecast by the Primitive Equation (PE) model of the National Meteorological Center (NMC).

Two versions of the method are available--an automated one that uses input data directly from the PE model and a manual one that can be used at forecast offices and depends on pressure forecasts from any source.

Experience has emphasized the importance of accurate input sea-level pressure forecasts. Indications are that the system is useful. Plans are to expand it to include other locations.

INTRODUCTION

The coastal storm of early March 1962 affected the entire Atlantic coast of the United States and produced record breaking high tides at locations between Long Island and Cape Hatteras. This storm was the most devastating extratropical storm on record, as it caused damage estimated to be over $200 million. Figures 1 and 2 show some of the damage at Virginia Beach, Va., and Rehoboth Beach, Del. It is fortunate that storms causing this much damage are rare. However, storms of lesser damage potential occur several times each winter. Accurate and timely forecasts of flooding and beach erosion caused by these storms are important. The crucial time to forecast these conditions is also the time when forecasters already have burdens brought on by poor weather conditions associated with coastal storms. It is therefore desirable to develop objective techniques for forecasting extratropical storm surges and to have these techniques computerized with meteorological data input from automated atmospheric prediction models.

CHARACTERISTICS OF THE EXTRATROPICAL STORM SURGE

Storm surge is the meteorological effect on sea-level and is computed as the algebraic difference between the observed tide and the normal astronomical tide. Figure 3 illustrates this definition with a 2-day tide record. The observed storm tide is shown by the upper solid curve, the normal (or predicted) astronomical tide by the dashed line, and the storm surge by the lower curve.

The frequency of significant storm surges varies from year to year. The average frequency of surges for eight locations is illustrated in figure 4. This graph is based on the data for the months of November through April during the years 1956-69. The recurrence of three classes of surge is shown--2 feet or greater, 3 feet or greater, and 4 feet or greater. For example, New York experiences a 2-foot surge or greater about six times per year. A 4-foot or greater surge occurs only about once every 2 years.

Factors that are important in determining the height of the storm tide are:

1. Astronomical tide,
2. Wind stress,
3. Atmospheric pressure effect,
4. Transport of water by waves and swell,
5. Effects of coastline configuration and bathymetry.

Astronomical Tide

The astronomical tide, caused by the difference in gravitational attraction of the sun and moon on the solid earth and the water of the oceans, is a major component of storm tides. By considering the mass of the sun to be 27 million times that of the moon and the sun's distance from earth to be 389 times that of the moons distance, the moon's tide generating force is calculated to be 2.17 times that of the sun.

There is a noticeable tide cycle during the synodic month, which is the 29.5-day interval between conjunctions of the sun and moon relative to the earth. The tide during the synodic month ranges from maximum at time of spring tide to minimum at time of neap tide. Spring tides occur when the moon is in conjunction or opposition to the sun relative to the earth (new moon and full moon). Neap tides, with less than normal range, occur at quadrature (first and last quarter moon phases). The position of the moon in its orbit around the earth also has an effect on the range of the tide. At perigee, when the moon is at its closest point to earth, the tide range is increased. The opposite condition exists at time of moon's apogee. These effects of relative position of the earth, moon and sun are illustrated in figure 5 from the U.S. Navy Glossary of Oceanographic Terms (1966).

The phase of the astronomical tide at the time of a meteorologically produced water level anomaly is important. If an anomaly occurs at time

of astronomical high tide, the resulting storm tide will be higher than if the anomaly occurs at time of astronomical low tide. This is illustrated in figure 6, where identical anomalies (storm surges) are combined with two different phases of astronomical tide. The anomaly combined with high astronomical tide results in a higher actual tide than the anomaly combined with low astronomical tide. It is generally assumed in storm tide calculations that the total storm tide is the algebraic sum of the storm surge or water level anomaly and the astronomical tide. Occasionally, interaction effects cause this assumption to be not perfectly valid. In these cases the surge determined by subtraction of the astronomical tide shows oscillations with approximately the same period as the astronomical tide. These oscillations are caused by a change in speed of the astronomical tide due to a change in the water depth. This change in water depth is caused by the storm surge. Examples of these secondary oscillations in the storm surge will be shown in later sections of this report.

Wind Stress

The rise of water caused by the action of the wind can be thought of as consisting of two components--that caused by the onshore wind component and that caused by the wind oblique to the shore. These two effects are illustrated in figures 7 and 8 (Harris 1963). The component caused by the onshore wind (fig. 7) is directly proportional to the wind stress and inversely proportional to the water depth. The other component, the effect of wind oblique to shore (fig. 8), comes from the wind-generated current which is parallel to shore. The effect of the earth's rotation is to have water piled up along the shore if the shore is to the right of the current.

Atmospheric Pressure Effect

The rise of the surface of the ocean in an area of low atmospheric pressure has been called the inverted barometer effect. This effect amounts to about a foot rise of sea level for an atmospheric pressure drop of 1 inch of mercury.

Transport of Water by Waves and Swell

Theory and laboratory experiments indicate that waves breaking near the shore contribute to the storm surge. Harris (1963) reported agreement by various investigators, that the slope of the water surface near shore is directly proportional to the square of the wave height and inversely proportional to the depth. This process is illustrated in the upper portion of figure 9 (Harris 1963).

Effects of Coastline Configuration and Bathymetric Conditions

The bottom topography near the shore is extremely important in determining the amplitude of the storm surge. Gentle sloping offshore bottom topography on the continental shelf supports the generation of higher storm surges than does a steep continental shelf. In the numerical calculation of storm surges, Jelesnianski (1972) has determined correction

factors for standard storm surges as a function of depth profile. These factors varied from about 0.5 to 1.5 for locations examined along the East Coast.

The configuration of the shore also has an effect on the resulting storm surge. There will be divergence of wave energy in coastal indentations such as coves and convergence of energy at coastal headlands or points. This effect leads to higher surges in areas of convergence as compared to areas of divergence. This effect is illustrated in the lower portion of figure 9.

RELATED STUDIES

Methods of forecasting storm surges have been put into three classes by Groen and Groves (1962). They are (1) empirical, (2) semi-empirical, and (3) theoretical. In the first class, direct relationships between meteorological variables at a point or over an area during some time period and the resulting storm surge are determined. Forecast methods of the second class are based on theoretical calculations, direct correlation, and perhaps some smoothing procedures. The theoretical approach is the numerical integration of the basic equations of motion and continuity.

An interesting comparison between the empirical and theoretical approaches has been made by Harris (1962). He pointed out that the two methods are not entirely independent, as the theoretical models often contain terms that must be determined empirically. Proper use of the empirical method calls for physical reasoning in selecting possible predictors for statistical models. Harris described the advantages of each method. Briefly, the theoretical approach can be generalized toward a better description of nature and can reveal useful information about the physical processes. The empirical approach does not reveal the physical processes as well as the theoretical approach, nor can it be generalized as well to describe natural processes. However, a forecast method derived empirically leads from the predictor data to the forecast by a much shorter route than one developed theoretically. Also, an empirical approach usually makes the most efficient use of the available data.

An important point, discussed by Harris, is that in developing a forecast method by either approach, the quality and quantity of input data available under operational conditions should be considered. A perfect computation scheme, without the required input data, would be of little use for operational forecasting.

Because the empirical approach was used in the present study, only previous studies of that type will be included in the following discussion.

Hustead (1955) developed an empirical method of forecasting the meteorologically produced tide departures from normal astronomical tide for the Norfolk, Va. tidal basin for northeast winds. This method is applicable to storms moving northward off the Virginia Capes, east of Cape Henry and Cape Charles. Figure 10 shows the tide departure as a function of mean

wind movement in a 2-hour period. Instructions for using the mthod, as given by Hustead (1955) are: "In practice, forecast the wind movement expected on triple register for the 2-hour period prior to hurricane or coastal wave center reaching latitude 37°N. Then divide this forecast wind value by two. With this value located along the abscissa, read the ordinate value of tidal departure on curve. This tidal departure value is then added to the normal tidal value predicted for the USC&GS Sewell's Point gage for the forecast time of the storm center to reach 37°N. This tidal height and time is the forecast occurrence for Sewell's Point and is then modified for any particular point in the tidal basin by using the time and height differences given in 'Table 2 - Tidal Differences and Ranges' as published in Tide Tables East Coast, North and South America (Including Greenland), U.S. Department of Commerce, Coast and Geodetic Survey."

Tancreto (1958) reasoned that since the Sverdrup-Munk-Bretschneider method of forecasting the height of significant wind-waves represents the transfer of energy from the wind to the waves, there should be some relationship between the forecast wave height and the magnitude of the storm surge. Based on 45 storms, the following regression equation relating the maximum height of the extratropical storm surge (S_h) to the forecast significant wave height (H), was derived for Boston:

$$S_h = 0.24 + 0.11\ H$$

where both S_h and H are expressed in feet. The correlation coefficient is 0.88.

Figure 11 is a scatter diagram showing the points on which this relationship was established, along with some independent cases. This equation is based on, and is applicable to, storms with strong winds with an easterly component along and off the southern New England coast. Stratification of the cases into two classes, those with east wind components and those with northeast wind components did not significantly improve the relationship.

Miller (1957) studied the effect of geostrophic wind over an offshore circular area 300 miles in diameter on the Atlantic City water level during a 6-month period. He concluded that the surge is nearly proportional to the wind speed, that in general there is a time lag of about 12 hours between the wind and the surge, and that maximum surge occurs with east-northeast winds.

The effect of extratropical storms on the tide at several Atlantic Coast stations was studied by Donn (1958), who generally agreed with Miller that the relationship between wind speed and surge seems to be linear, and that there is a time lag between the wind and the storm surge.

The Storm Tide Warning Service of the United Kingdom Meteorological Office has an operational method for forecasting storm surges on the North Sea coasts of England and Scotland. Hunt (1972) reported that a system

of surge-prediction formulae has been developed for eight locations. The formulae are applied at 12 and again at 4 hours before normal high tide and yield forecasts of storm surge at time of high tide. Geostrophic wind over 5 circular areas of 60-nautical-mile radius over the western portion of the North Sea are input data to the forecast equations. Also, prior storm surge values to the north (upstream) are included as predictors. The method has been quite successful.

DEVELOPMENT OF THE METHOD

The method is a statistical one that relates meteorological data to the storm surge. The wind is certainly the meteorological variable which generates nearly all the storm surge. Several studies have shown relationships of surface wind conditions at coastal weather stations to the surge (Pore 1964, 1965). Information available from the Primitive Equation (PE) model at the National Meteorological Center (NMC) favors the use of meteorological data at computation grid points rather than at weather stations. For that reason, sea level pressure forecasts at specific grid points were used to represent the generating winds off the East coast in the storm surge generation process. NMC runs its Primitive Equation model, which produces meteorological forecasts for most of the Northern Hemisphere, every 12 hours.

The storm surge forecast technique is based on data for 13 winters (November through April) from 1956 to 1969. The data for eight east coast stations covered by this period were examined. The storms causing surges of 2 feet or greater at four or more of these stations were included in this study. The tracks of the 68 storms which met this requirement are shown in figure 12.

The NMC computation grid points, where sea-level pressure was considered as possible predictors of storm surge, are shown in figure 13. Sea-level pressure values at these grid points were obtained at 6-hour intervals from analyzed weather charts for the 68 storms. These pressure values, with appropriate time lags, were considered as possible predictors of the storm surge.

Forecast equations were derived by the statistical screening procedure, which has been described by Klein (1965) as follows:

> "The object of the screening procedure is to select from a large set of possible predictors only those few which contribute significantly and independently to the forecast of a predictand. This is accomplished by a forward method of multiple regression in which significant predictors are picked in a stepwise fashion, one by one. As a result, a small number of predictors can be selected which contain practically all the linear predictive information of the entire set with respect to a specific predictand. The importance of using a small set of predictors to prevent redundancy and instability of the multiple regression equation

and to insure good results when applying it to new data has been emphasized by Lorenz (1956, 1959), Grant (1956), Panofsky and Brier (1958), and others."

A detailed description of the selection of predictors by screening is given by Miller (1958). The manner in which predictors of storm surge are screened is shown below:

1) $SS = A_1 + B_1X_1$

2) $SS = A_2 + B_2X_1 + C_1X_3$

3) $SS = A_3 + B_3X_1 + C_2X_2 + D_1X_3$

.

.

.

n) $SS = A_n + B_nX_1 + C_{n-1}X_2 + \ldots + NX_n$

where SS is storm surge, A_1, A_2, A_3, etc., are constants, X_1, X_2, X_3, etc., are predictors, and B_1, B_2, C_2, etc., are regression coefficients.

The procedure is to first select the best single predictor (X_1) for regression equation 1. The second regression equation contains the first predictor (X_1) and the predictor (X_2) that contributes most to reducing the residual after the first predictor is considered. This screening procedure is carried out until the desired number of predictors is included or until the additional variance explained by adding predictors reaches some cutoff value.

THE FORECAST EQUATIONS

The following data were used in the derivation of the storm surge forecast equations with the statistical screening procedure:

1. Six-hour values of storm surge at the 10 locations are shown in figure 14. These locations were chosen because they are in densely populated areas which are frequently threatened by extratropical storm surges. Also, accurate tide observations, necessary for verification of forecasts, are available for these locations from the National Ocean Survey and the U.S. Army Corps of Engineers.

2. Sea-level pressure at the 75 grid points at 6-hour intervals for 68 storms during the winters of the period 1956 - 1969. These storms caused surges of 2 feet or more at 4 or more of the 10 stations.

Screening regression runs were made separately for each location so that the local effects of coastline configuration and bathymetry are considered. The particular storms that affected the respective stations by causing 2 feet or more of surge were included for processing by the screening program. Out of the total of 68 storms, the number used in the screening process varied from a maximum of 58 for Atlantic City to 30 for Hampton Roads.

The screening process was done in two parts for each location. First, 7 screening runs were made using the pressure at all 75 grid points, 1 for each lag time from 0 hours to 36 hours at 6-hour intervals. Then the first few predictors selected for each of these runs were combined to make up the predictors of the final screening run.

Data were available for only a couple of years for Stamford, Conn. and as a result, only eight storms were used in deriving the Stamford equation. This equation will be re-derived when more data are available.

The format of the storm surge equation for New York is shown in figure 15. It includes predictors at eight grid points with time lags of 0 or 6 hours. These predictor terms were added one by one by the screening process until the next term explained less than 1% of the variance. The terms are shown in their order of selection. The first predictor selected was the pressure at point 47 with a negative coefficient. This indicates that a low pressure area in the Norfolk, Va., area would correlate well with high storm surge at New York, which is reasonable. The addition of the second term, pressure at point 17 with a positive coefficient, yields predictor information related to the pressure gradient between points 17 and 47. This pressure gradient is a good indicator of northeast wind in the New York area, a condition favorable for storm surge generation.

The first two terms selected for the other stations also indicated favorable pressure gradients for generation of storm surge. The addition of more terms adds significant prediction capability to the forecast equation, but the physical significance of the additional terms is often masked by the interdependence of the terms. In fact, the addition of several terms often will change the algebraic sign of predictor terms and further mask the physical significance.

Statistical forecast equations often tend to underforecast peak values if they are derived to give minimum root-mean-square errors for entire storms, rather than minimum error at only the peak values. This was true for the 10 storm surge forecast equations. The time of the peak surge was determined quite accurately but the heights of the forecasts were generally too low. Klein et al. (1954) have pointed out that this tendency can be corrected by "inflating" the forecasts so that the variability of the observed and forecast values is approximately the same. This adjustment was made such that the forecasts made by each original forecast equation were multiplied by the reciprocal of the correlation coefficient between the storm surge and the predictors. Actually the adjustment was made by changing the coefficients and constants in each equation. The adjusted forecast equations are

shown in appendix A. Table 1 contains the statistics for the forecast equations, where they are referred to as automated equations. Table 1 also contains statistics for manual equations that will be described in a later section.

APPLICATION TO PAST STORM CASES

The storm surge forecast method did not become operational until October 1971. However, it was desirable to test the method on several intense storms that occurred prior to that time. This was done by using sea-level pressure analyses as input data instead of pressure forecasts.

Storm surge calculations were made for seven storms with analyzed pressure values as input. Included were the famous storms of November 1950 and November 1953 that caused severe flooding and extensive damage in the New York and New England areas and the storm of March 1962 that affected the entire East coast. Calculations were made for four other storms that occurred in March 1957, January 1966, and November 1968. These cases were selected because they caused significant storm surges in most of our area of interest.

For each of these storms we have prepared figures showing a series of synoptic charts and graphs of the observed storm surge and the calculated values of storm surge. The observed storm surge curves are based on hourly values and are shown by the solid lines. The maximum storm surge values are printed near the peaks of these curves. The dashed lines connect the computed values of the storm surge which are made at 6-hour intervals. The dates are placed at the 1200 EST positions. Wind observations at coastal stations are shown for some of the storms. These were obtained from many issues of Local Climatological Data.

Storm of November 25-26, 1950

This storm was considered by some to be the worst on record for the eastern United States (Bristor 1950 and Smith 1950). It caused severe cold, heavy rain, deep snow, destructive ice accretion, high winds, and extremely high storm surges along the northeast coast. The storm occurred near the time of spring tide, as full moon occurred on November 24.

The storm first appeared on the surface weather chart for 1230 GMT November 24 as a low on a cold front over North Carolina and Virginia. The low deepened considerably before a new low formation became evident near Erie, Pa. at 1530 GMT November 25 (Smith 1950). This new center became the main storm and at 0030 GMT of November 26 was near Cleveland, Ohio with central pressure of 983 mb. The lowest pressure of 978 was reached at 0630 GMT November 26. The storm subsequently moved northward. Figure 16 shows a series of sea-level pressure patterns from 0130 EST November 24 to 1330 EST November 26. Wind values that occurred at some coastal locations during this storm are shown in table 2 (U.S. Department of Commerce 1950).

This was a very unusual storm in a storm surge sense. The strong winds were more easterly and southeasterly in contrast to the usual northeast winds of extratropical storms in this area. The sea-level pressure charts (fig. 16) indicate the long fetch important in storm surge generation. The situation was complicated by the passage of a frontal system over the coastal area. For example, the wind at La Guardia Airport shifted from ESE to SSW with the frontal passage around 1800 EST on November 25.

New record high tides were recorded at the following locations, as indicated in an index of tide gage record by Harris and Lindsay (1957):

Port Chester, N.Y.
Shinnecock Inlet, Long Island
Oak Beach, Long Island
Freeport, Long Island
Jones Inlet, Long Island
Brooklyn, N.Y. (Hudson Ave. and East River)
New York City (15th St. and East River)
Spuyten Duyvil, NYC, (Hudson and Harlem Rivers)
Sherman Creek, 201st St. and Harlem River, NYC)
Elm Park, Staten Island
Arthur Kill (Staten Island), NYC
East Newark, N.J. (Passaic River)
Caven Point, N.J. (Upper N.Y. Bay)
Perth Amboy, N.J. (Raritan Bay)
South Amboy, N.J. (Raritan Bay)
New Brunswick, N.J. (Raritan River)
Sayreville, N.J. (Raritan River)
Red Bank, N.J. (Navesink River)
Branchport, N.J. (Shrewsbury River)
Manasquan Inlet, N.J.
Philadelphia, Pa. (Pier 9 - North)
Deep Water, N.J. (Chambers Works Plant of duPont)
Cambridge, Md.

The storm surge records shown in figure 17 have considerable oscillations near the time of maximum surge. This is probably an interaction effect where the speed of the astronomic tide is changed as a result of the changing depth caused by the storm surge.

Maximum storm surges were 8.1 feet at Willets Point, N.Y. and the Battery in New York City. The highest actual water levels at these locations occurred about 3 hours before the peak storm surge at Willets Point and about 6 hours before the highest surge at New York City. The highest water levels occurred near the time of high astronomical tide. The times of high astronomical tide are indicated by arrows near the storm surge curves.

This storm was the one extratropical storm in this geographic area of recent decades to differ considerably from the cases used in developing the storm surge forecast method. The calculations of storm surge, shown by the dots in figure 17, did not show the peak surge to be high enough; however the overall surge calculations are not too bad.

Storm of November 6-7, 1953

At many places the storm of early November 1953 produced the heaviest snowfall of record for so early in the season. The largest reported amount was 27.5 inches at Middleburg, Pa. (Fulks 1953). The storm also caused strong onshore coastal winds with speeds approaching those of the famous 1950 storm.

Surface pressure charts are shown for a period from November 6 to November 8 in figure 18. The low had formed in the northeastern Gulf of Mexico and by 0130 EST on the 6th was located just off the Georgia-Florida coastal area. It progressed to the Cape Hatteras area by 1330 EST on the 6th, to the Delaware area by 0130 EST on the 7th. The storm crossed Long Island and was over New York State at 1330 EST on the 7th. The pressure gradient resulting from the low pressure of the storm and the strong high located over the Great Lakes area caused extremely high winds north of the storm center. These winds caused high storm surges with considerable flooding and flood damage along the Middle Atlantic and New England coasts.

Wind observations for some coastal stations are shown in table 3. Atlantic City experienced fastest mile wind of 69 mph and Boston had a fastest mile of 67 mph. The observed storm surges and the calculation of surges, with sea-level pressure analyses as input, are shown in figure 19. Peak surges at Willets Point and the Battery were 7.6 and 5.4 feet, respectively. These are extremely high values for storm surge and unfortunately the calculated surges for these locations are too low. The surge calculations are in good agreement with the actual surges at the other locations.

Storm of March 8-9, 1957

The storm of March 8-9, 1957 closely followed the coast north of Cape Hatteras (fig. 20) and caused storm surges of about the same magnitude at all of our locations of interest (fig. 21). Peak surge values at all nine locations ranged from 2.1 to 2.4 feet. Fastest mile wind at Boston was from the northeast at 45 mph (table 4).

Storm of March 5-8, 1962

The waves and storm tides generated by the storm of March 5-8, 1962 caused unprecedented damage to coastal areas form southern New England to Florida. The very persistent strong northeast winds blowing over an extremely long fetch were responsible. Another important factor is that the storm occurred at a time of very high astronomical tide. Articles by Stewart (1962) and Cooperman and Rosendal (1962) give details of the storm.

At 7 a.m. EST on March 5th there was an ill-defined low pressure area with a frontal wave northeast of the Bahamas. Low pressure also extended northwestward through the Carolinas and Virginia. By 7 a.m. EST on the 6th

the entire low pressure area had deepened, resulting in a long easterly fetch over the western Atlantic north of Cape Hatteras. The storm continued to intensify and resulted in an elongated low with strong northeast wind over a very long fetch. Six pressure analyses for the storm are shown in figure 22.

It was a rare coincidence that a storm of such magnitude with a long northeasterly fetch would coincide with spring tide. However, this was the case. Not only did the storm occur at spring tide but it occurred at the time of the moon's perigee--the time when the moon is nearest to the earth. Therefore the storm occurred at the time of perigee spring tide, which is close to maximum astronomical tide.

Some of the higher wind gusts at coastal stations were:

Portland, Maine	NE 43 mph;
Cape Cod Canal, Mass.	NE 73 mph;
Nantucket, Mass.	NE 69 mph;
Block Island	NE 84 mph;
Chesapeake L.S.	NNE 80 mph;
Nags Head, N.C.	76 mph.

Other wind observations are given in table 5.

Several agencies such as the Geological Survey, the Corps of Engineers, and the Coast and Geodetic Survey collected observations of high water marks following this storm. Variations in maximum water levels of 2 to 4 feet were found within a distance of a half mile (Harris, 1963). This was the first extratropical storm in which high water marks were observed sufficiently close together to show this large variation.

Maximum storm surge values were high on the northeast coast with 6.0 feet being observed at Breakwater Harbor, Del. and 5.6 feet being observed at Hampton Roads, Va. (fig. 23). This was one storm in which the timing of the surge was not very important because the surge became high and stayed high through about five high tide cycles.

Calcuations of the surges (fig. 23), based on sea-level pressure analyses, are in good agreement with the observed surges. The observed surge curve for Willets Point is a good example of the interaction between the storm surge and the astronomical tide.

Storm of January 23-24, 1966

The storm of January 23-24, 1966, resulted in heavy snow over most of New England and high tides that caused considerable damage along the northeast coast. The low developed in the eastern Gulf of Mexico, moved northeast, and was near Cape Hatteras at 0100 EST January 23 (fig. 24). It subsequently moved northeastward away from the coast. Wind observations for several locations are shown in table 6. Calculations of the storm surge shown in figure 25 are in good agreement with the observed storm surges.

Storms of November 10 and November 12, 1968

Two storms affected the tide during the period November 9-13, 1968. The first developed in the Gulf and moved northeast along the coast in a typical manner (fig. 26). Significant storm surges were observed on Nov. 10, as shown in figure 27. On November 11 the next storm developed and followed a similar path (fig. 28). It was the largest and most damaging storm in several years to affect the east coast (U.S. Department of Commerce 1968). Wind values for both storms are shown in table 7. The high tides and 30-foot breakers caused hundreds of residents to evacuate their homes. Peak wind gusts were 60 mph at New York and over 100 mph at Wallops Island, Va. Damage to coastal areas from New England to North Carolina were estimated in millions of dollars. Storm surge calculations for both of these storms are in good agreement with the observed surges (fig. 27).

OPERATIONAL USE OF THE METHOD

For operational use, sea level pressure forecasts at the appropriate grid points are used as input to the storm surge equations. The pressure forecasts are available twice daily from the PE model of NMC. Pressure forecasts at 6-hour intervals to 48 hours are used.

A sample teletype bulletin of storm surge height forecasts for the 10 locations is shown in figure 29. The forecasts are expressed in feet at time intervals of 6 hours for the 48-hour forecast period. Such messages are transmitted on a National Weather Service teletype circuit to forecast offices along the East coast where they are used as guidance in preparing the official storm tide bulletins.

Soon after the automated forecast method became operational, two extra-tropical low pressure systems moved up the east coast of the United States, the first on February 4, 1972. This was followed by a more intense system on February 19. The two storm surge cases associated with these systems are discussed below.

February 4, 1972

A low pressure system which developed near the South Carolina coast and moved rapidly northeastward is depicted in figure 30. Storm surge calculations, based on sea-level pressure analyses of the NMC Northern Hemisphere surface charts, are shown in figure 31. The observed storm surges, based on hourly values, are shown by solid curves. Calculations of the storm surge, based on pressure analyses are shown by dots at 6-hour intervals. In the same manner, figures 32, 33, and 34 show actual forecasts of surge based on the sea-level pressure forecasts. These three figures show the 6-, 12-, 18-, 24-, 30-, and 36-hour forecasts of the surge. Two forecasts were combined on each chart so that there is a forecast value every 6 hours, rather than every 12 hours. The forecasts were quite good.

February 19, 1972

A low pressure system centered over the Great Lakes at 0700 EST on February 18 had a frontal system extending southward over eastern Tennessee, Georgia, Alabama, and into the Gulf of Mexico. Subsequent developments, as depicted on the Northern Hemisphere surface charts of NMC, are shown in figure 35. By 1300 EST, a closed low had developed over Georgia. Further development occurred and the storm moved rapidly toward the north-northeast, to a position just north of Cape Cod at 0100 EST on the 20th. Some wind velocities for Weather Service stations, as recorded in the Environmental Data Service publication, Local Climatological Data, are shown in table 8.

Some of the PE model forecasts of storm position and central pressure are shown in figure 36. The storm center positions and central pressures taken from the NMC Northern Hemisphere surface charts can be compared to these 12-hour, 24-hour, and 36-hour forecasts. The shorter range numerical forecasts of the track were consistent with the longer range forecasts and are considered to be quite good.

The numerical sea-level pressure forecasts, valid about the time of maximum storm surge, can be compared to the NMC pressure analysis in figure 37. Here it is seen that the longer range forecasts, such as the 30-hour forecast, underestimated the storm intensity. The shorter range forecasts, such as the 6-hour forecasts, look quite good for both storm intensity and position.

Calculations of the storm surge based on sea-level pressure analyses and forecasts are shown in figures 38 through 41. Storm surge calculations based on sea-level pressure analyses of the NMC Northern Hemisphere surface charts are shown in figure 38. Here the observed storm surges, based on hourly values, are shown by the solid curves. Calculations of storm surge, based on pressure analyses, are shown by the dots at 6-hour intervals. It is felt that these storm surge calculations agree fairly well with the observations. In the same manner, figures 39, 40, and 41 show actual forecasts of surge based on the sea-level pressure forecasts. These three figures show 6-, 12-, 18-, 24-, 30-, and 36-hour forecasts of the surge. Two forecast intervals are combined on each chart so that there is a forecast value every 6 hours rather than every 12.

The actual forecasts of storm surge, of course, are not as accurate as the calculations based on the pressure analyses. The underforecasting of storm intensity by the PE model in the longer range forecasts was discussed earlier and is reflected in the longer range forecasts of storm surge, as shown in figure 41. The 6- and 12-hour surge forecasts were closer to the observed surge than the longer range 30- and 36-hour forecasts. The automated storm surge forecasts provided useful guidance material, especially on the timing of the surge.

MANUAL FORECAST METHOD

There are several reasons why a manual forecast method for storm surges is desirable in addition to the automated method. There are times when the

automated storm surge forecasts are not received at forecast offices because of computer problems or communication difficulties. At such times a hand-computed forecast can serve as a substitute. There may be other times when a forecaster does not agree with the sea-level prognoses of the numerical weather model, which are used as input for automated storm surge forecasts. When this occurs, a forecaster may calculate a surge forecast, using his own prognoses of the sea-level pressure pattern.

The manual method consists of a set of regression equations derived in a manner similar to that of the automated method. The differences are that the predictors are sea-level pressures with zero time lags rather than with variable time lags. Also, only a few terms are included in each regression equation. Table 1 contains the statistics for the manual method. Comparison of the statistics for the automated method shows a slight loss of correlation for most stations and a moderate loss for the Chesapeake Bay locations. This points out the importance of longer lag times of the wind for generating Chesapeake Bay surges.

The manual forecast equations are shown in appendix B. Here the point numbers are identified in the same manner as they were in the automated method (fig. 13). The determination of the various terms of the forecast equations can be done once and for all over a suitable range of pressure and put into table form for convenient use. This reduces the calculations of the manual method to table lookup and addition. Such a table and a calculation form have been prepared for Boston, and could be prepared for the other locations.

Table 9 shows the values for manual storm surge calculation at Boston. The forecast equation at the top of the table is for storm surge expressed in feet and the predictor pressures expressed in millibars. The forecast is valid for the same time as the predictor pressure values (zero time lag). The equation uses pressures at five of the NMC grid points which are re-named A, B, C, D, E for convenience. The values in the table labeled B', C', D', and E' are the products of the coefficients and the pressure values as shown in the regression equation. The value A' is also a product with the regression constant added. Figure 42 contains a map showing the location of the predictor points for storm surge at Boston and a calculation form.

Consider the pressure analysis for 1300 EST February 19, 1972 (fig. 43) as an example. The pressure at point A is 989 mb , which gives a value of 41.55 from table 9. The same procedure is used to determine the value of B', C', D', and E'. The sum of these five terms gives a storm surge calculation of 3.1 feet for Boston, as shown in figure 42. Figure 44 shows the calculated surges based on the sea-level pressure analyses for both the automated and manual methods and the observed surge for the March 1962 storm surge case. Calculations by the manual method, shown by open circles, are similar to those by the automated method; both agree well with the observed surges.

CONCLUSIONS

The statistically derived extratropical storm surge forecast methods use sea-level pressure forecasts as input to provide guidance material for Weather Service Forecast Offices. The accuracy of the surge forecasts depends greatly on the accuracy of the pressure forecasts. Experience so far has shown that the method provides useful guidance material.

Observed storm surges at New Bedford, Mass, and Providence, R.I., are very similar to observed storm surges at Newport, R.I. Therefore, the storm surge forecasts for Newport can be used as guidance in forecasting surges at New Bedford and Providence. Comparison of storm surges at other locations may show additional useful similarities.

Forecast equations will be derived for several additional locations. These will be tested and added to the automated system if appropriate.

ACKNOWLEDGEMENTS

Appreciation is expressed to the National Ocean Survey and the U.S. Army Corps of Engineers for the observed tide data. Appreciation is also expressed to Mr. R. E. Lynde of the Weather Service Forecast Office, Boston for his helpful suggestions, and to Mrs. Audrey Johnson for typing the manuscript.

REFERENCES

Bristor, C. L., "The Great Storm of November 1950, "Weatherwise, Vol. 4, No. 1, Feb. 1951, pp. 10-16.

Cooperman, A. I., and H. E. Rosendal, "Great Atlantic Coast Storm, 1962," Climatological Data, National Summary, Vol. 13, No. 3, U.S. Department of Commerce, March 1962, pp. 137-145.

Donn, W. L., "An Empirical Basis for Forecasting Storm Tides," Bulletin of the American Meteorological Society, Vol. 39, No. 12, 1958, pp. 640-647.

Fulks, J. R., "The Early November Storm of 1953," Weatherwise, Vol. 7, No. 1, Feb. 1954, pp. 12-16.

Grant, A. M., "The Application of Correlation and Regression to Forecasting," Meteorological Study No. 7, Bureau of Meteorology, Commonwealth of Australia, Melbourne, Jan. 1956, 21 pp.

Groen, P., and G. W. Groves, "Surges," Chapter 17 of The Sea, Vol. 1, John Wiley and Sons, Inc., 1962, pp. 611-646.

Harris, D. L., and C. V. Lindsay, "An Index of Tide Gages and Tide Gage Records for the Atlantic and Gulf Coasts of the United States," National Hurricane Research Project Report No. 7, Washington, D.C., May 1957, 104 pp.

Harris, D. L., "The Equivalence Between Certain Statistical Prediction Methods and Linearized Dynamical Methods," Monthly Weather Review, Vol. 90, August 1962, pp. 331-340.

Harris, D. L., "Coastal Flooding by the Storm of March 5-7, 1962," manuscript of the U.S. Weather Bureau, Washington, D.C., January 1963, 22 pp.

Hunt, R. D., "North Sea Storm Surges," The Marine Observer, Vol. XLII, No. 237, July 1972, pp. 115-124.

Hustead, A. D., "An Empirical Method of Forecasting Meteorological Produced Tidal Departures from the Normal Astronomical Tide in the Norfolk, Va., Tidal Basin for a Specific Wind Direction," manuscript of the U.S. Weather Bureau, Washington, D.C., August 1955, 5 pp.

Jelesnianski, C. P., "SPLASH (Special Program to List Amplitudes of Surges from Hurricanes) I. Landfall Storms," NOAA Technical Memorandum NWS TDL-46, April 1972, 52 pp.

Klein, W. H., B. M. Lewis, and I. Enger, "Objective Prediction of Five-Day Mean Temperature During Winter," Journal of Meteorology, Vol. 16, No. 6, Dec. 1959, pp. 672-682.

Klein, W. H., "Application of Synoptic Climatology and Short-Range Numerical Prediction to Five-Day Forecasting," U.S. Weather Bureau Research Paper 46, 1965, 109 pp.

Lorenz, E. N., "Empirical Orthogonal Functions and Statistical Weather Prediction," Statistical Forecasting Project Scientific Report No. 1, Contract No. AF19(604)-1566, Department of Meteorology, Massachusetts Institute of Technology, Cambridge, Mass., Dec. 1956, 49 pp.

_____, "Prospects for Statistical Weather Forecasting," Statistical Forecasting Project Final Report on Contract No. AF19(604)-1566, Department of Meteorology, Massachusetts Institute of Technology, Cambridge, Mass., 1959, pp. 1-78.

Miller, A. R., "The Effect of Steady Winds on Sea Level at Atlantic City," Meteorological Monographs, American Meteorological Society, Vol. 2, 1957, pp. 24-31.

Miller, R. G., "The Screening Procedure. Studies in Statistical Weather Prediction," Final Report, Contract No. AF19(604)-1590, Hartford, Conn., Travelers Weather Research Center, 1958, pp. 86-95.

Panofsky, H. A., and G. W. Brier, "Some Applications of Statistics to Meteorology," College of Mineral Industries, Pennsylvania State University, University Park, Pa., 1958, 224 pp.

Pore, N. A., "The Relation of Wind and Pressure to Extratropical Storm Surges at Atlantic City," Journal of Applied Meteorology, Vol. 3, No. 2, April 1964, pp. 155-163.

_____, "Chesapeake Bay Extratropical Storm Surges," Chesapeake Science, Vol. 6, No. 3, September 1965, pp. 172-182.

Smith, C. D., "The Destructive Storm of November 25-27, 1950," Monthly Weather Review, Vol. 78, No. 11, Nov. 1950, pp. 204-209.

Stewart, J. Q., "The Great Atlantic Coast Tides of 5-8 March 1962," Weatherwise, Vol. 15, No. 3, June 1962, pp. 116-120.

Tancreto, A. E., "A Method for Forecasting the Maximum Surge at Boston Due to Extratropical Storms," Monthly Weather Review, Vol. 86, No. 6, June 1958, pp. 197-200.

U.S. Dept. of Commerce, Climatological Data, National Summary, Vol. I, No. 11, November 1950.

U.S. Dept. of Commerce, Climatological Data, National Summary, Vol. 19, No. 11, November 1968.

U.S. Naval Oceanographic Office, Glossary of Oceanographic Terms, SP-35, Second Edition, Washington, D. C., 1966, 204 pp.

Figure 1. Property damage at Virginia Beach, Va., following the severe March 1962 storm.

Figure 2. Boardwalk destroyed at Rehoboth Beach, Del., by the March 1962 storm.

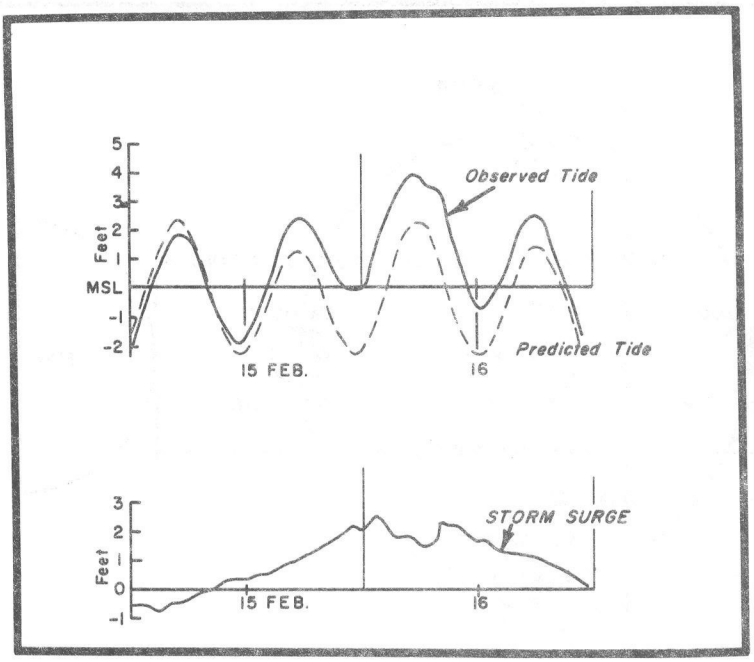

Figure 3. Example of tide data showing the observed tide, the predicted astronomical tide, and the storm surge.

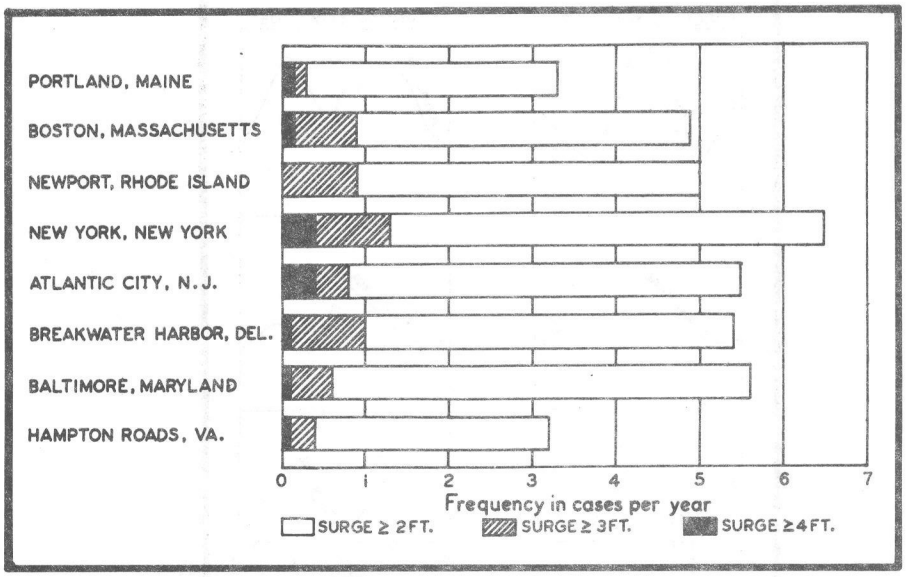

Figure 4. Frequency of extratropical storm surges equal to or greater than 2, 3, and 4 feet at eight locations from Portland, Maine to Norfolk, Va.

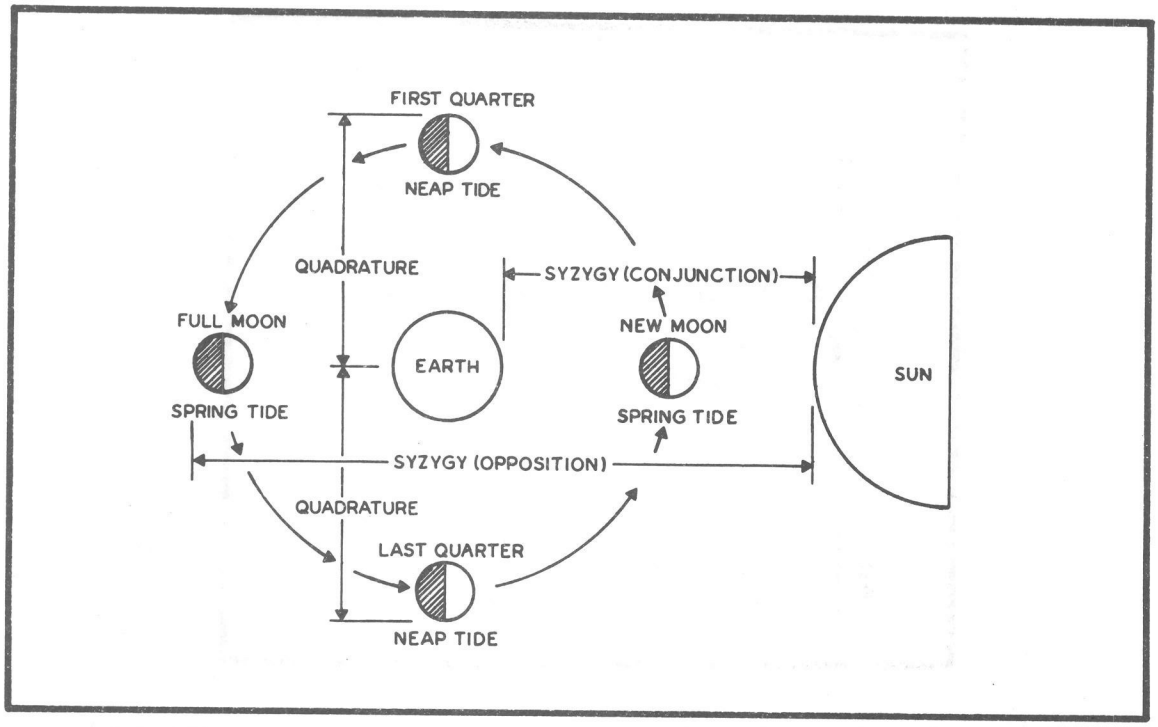

Figure 5. Diagram of lunar cycle responsible for tide cycle. From U. S. Navy Glossary of Oceanographic Terms (1966).

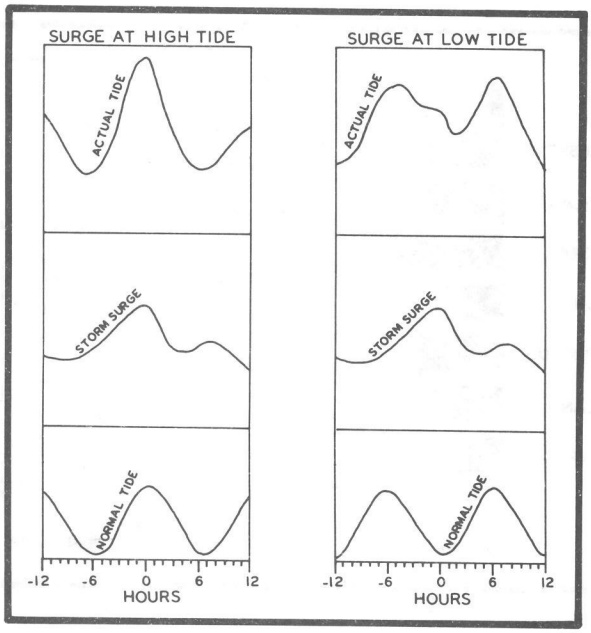

Figure 6. The actual tide and its components. The time of occurrence of the storm surge with respect to the normal tide is important in determining the height of the actual tide.

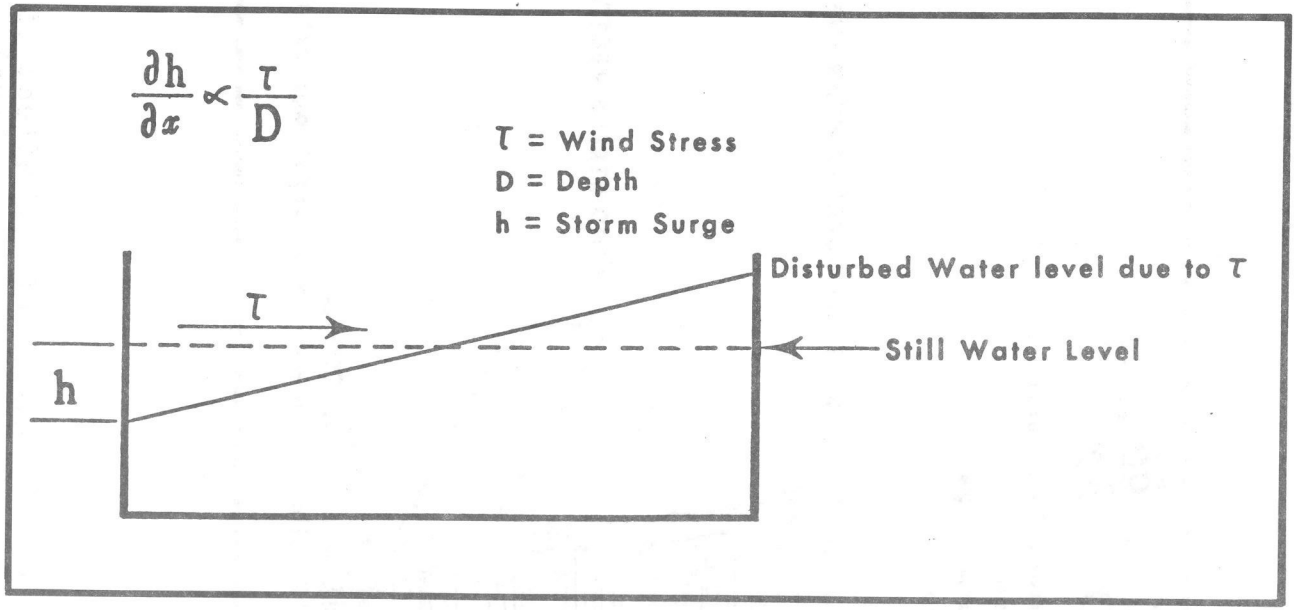

Figure 7. Schematic of the effect of an onshore wind on water level (Harris 1963).

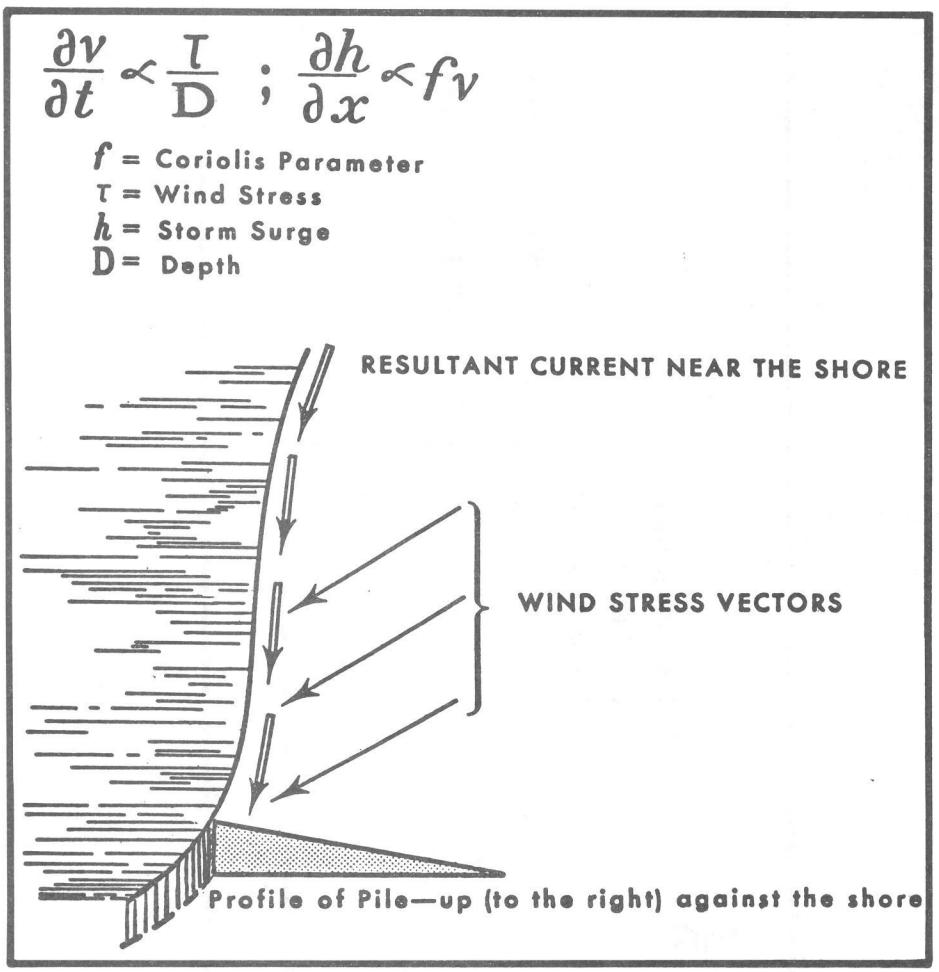

Figure 8. Schematic of the effect of an oblique wind on the water level (Harris 1963).

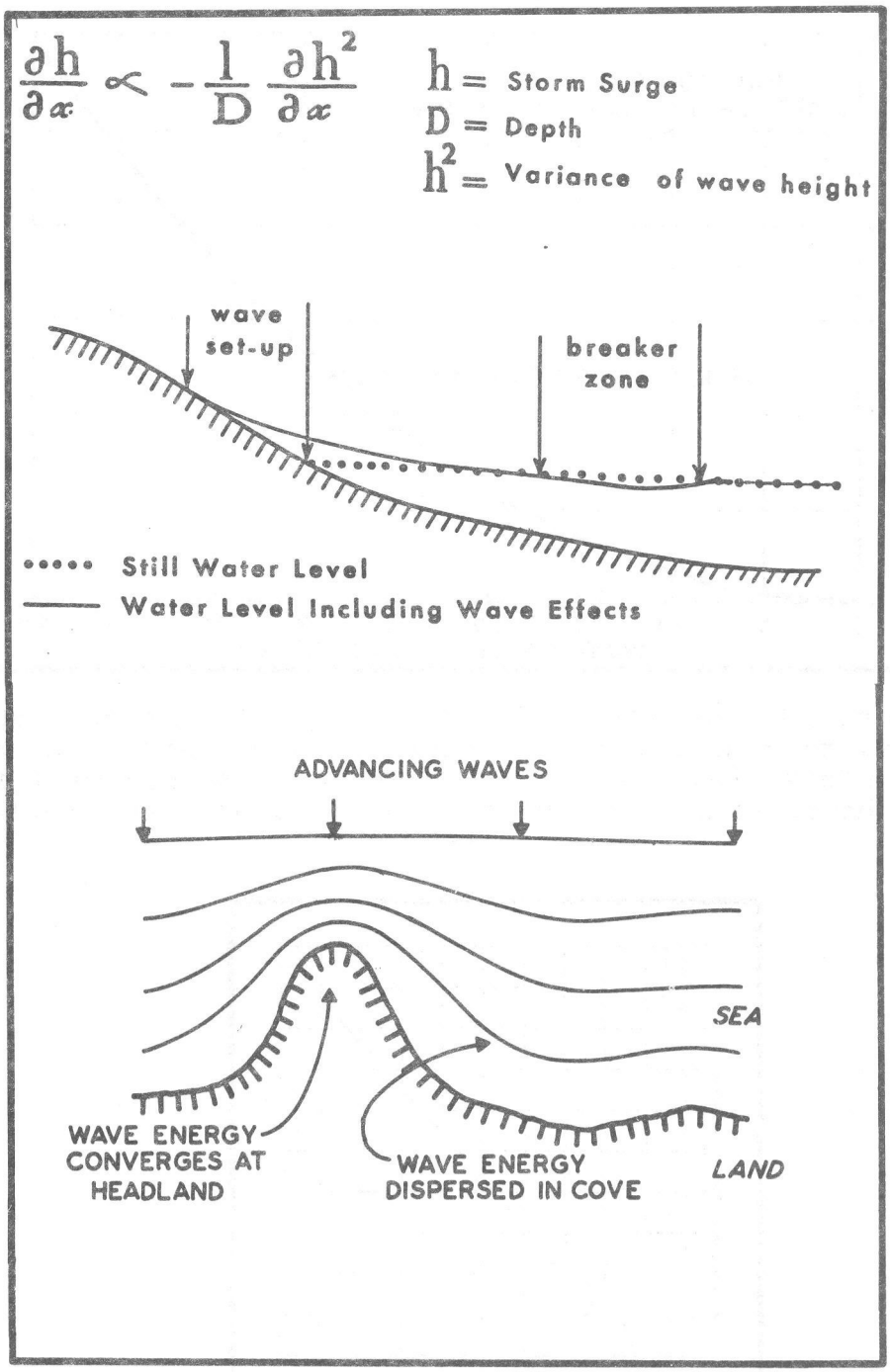

Figure 9. Schematic of wave set-up in a vertical plane (above) (Harris 1963) and in a horizontal plane (below).

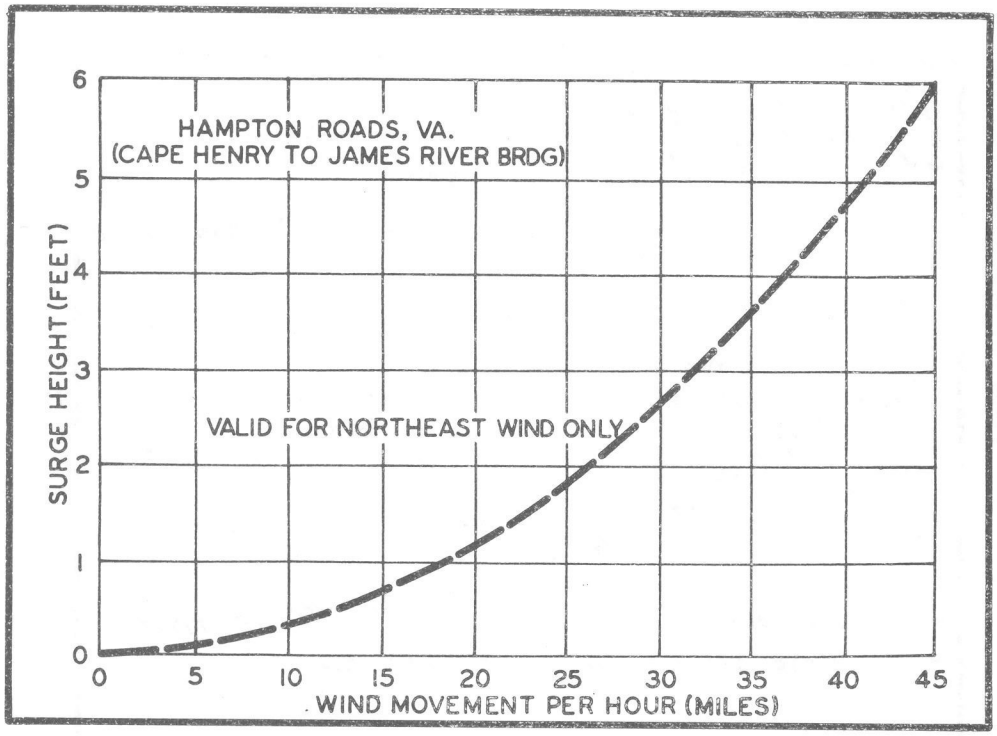

Figure 10. Relation of storm surge at Hampton Roads, Va. to 2-hour wind movement for northeast winds at Norfolk, Va. Values are based on mean movement for 2 hours prior to indicated tidal departure (Hustead 1955).

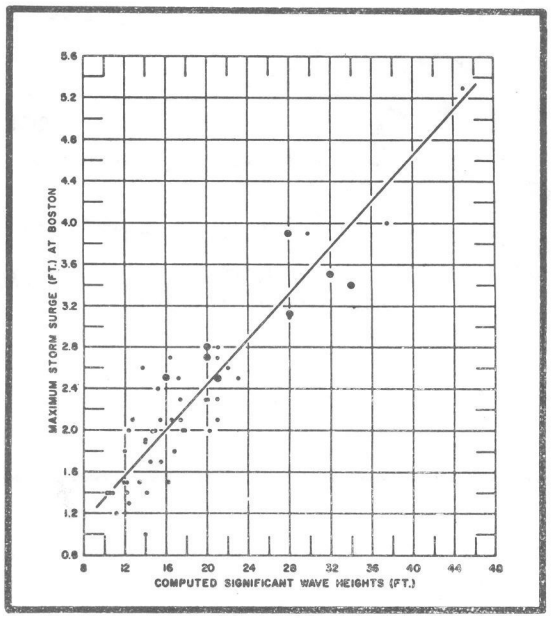

Figure 11. The maximum storm surge at Boston as a function of the computed offshore wave heights. The dependent data are plotted as dots and the independent data as encircled dots (Tancreto 1958).

Figure 12. Tracks of storms that produced surges of 2 feet or more at four or more of the forecast locations.

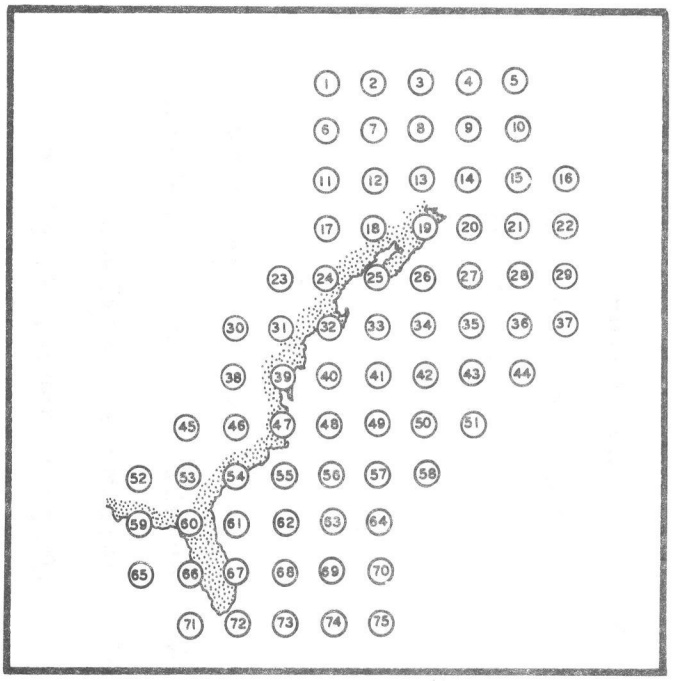

Figure 13. Computation points where predictors of storm surge were considered in the derivation of the forecast equations.

PWM Portland, Maine

BOS Boston, Massachusetts

NWP Newport, Rhode Island

LGA Willets Point, New York

SFD Stamford, Connecticut

NYC New York, New York

ACY Atlantic City, New Jersey

BWH Breakwater Harbor, Delaware

BAL Baltimore, Maryland

ORF Hampton Roads, Virginia

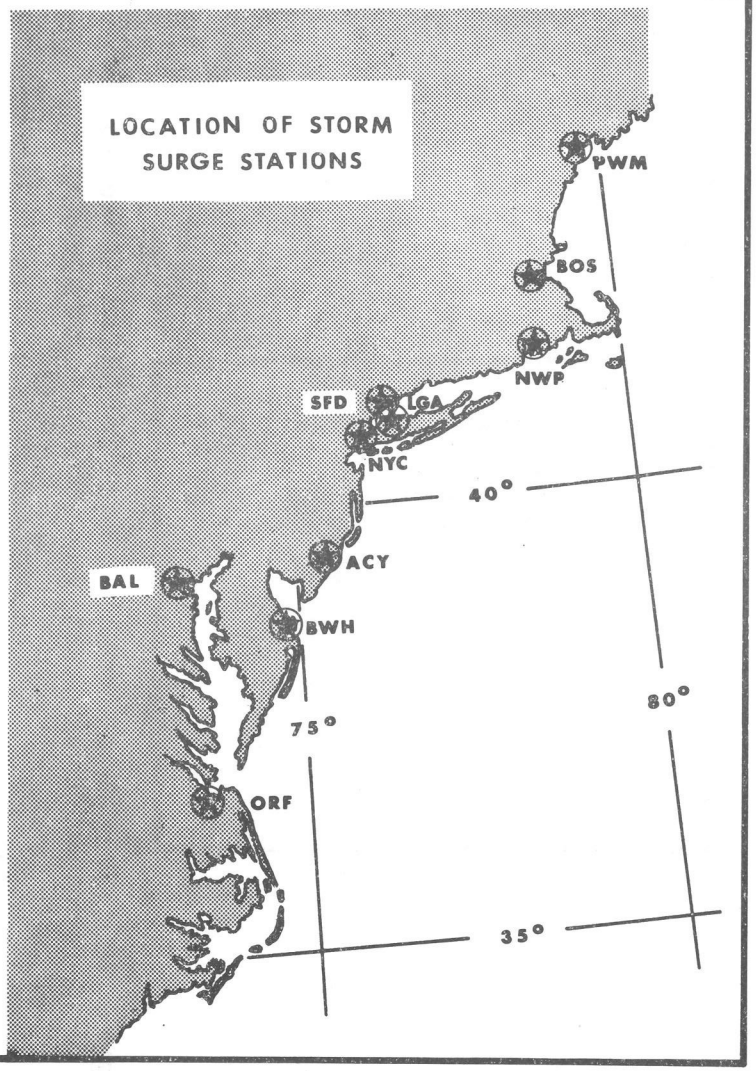

Figure 14. The 10 forecast locations for which storm surge equations were derived.

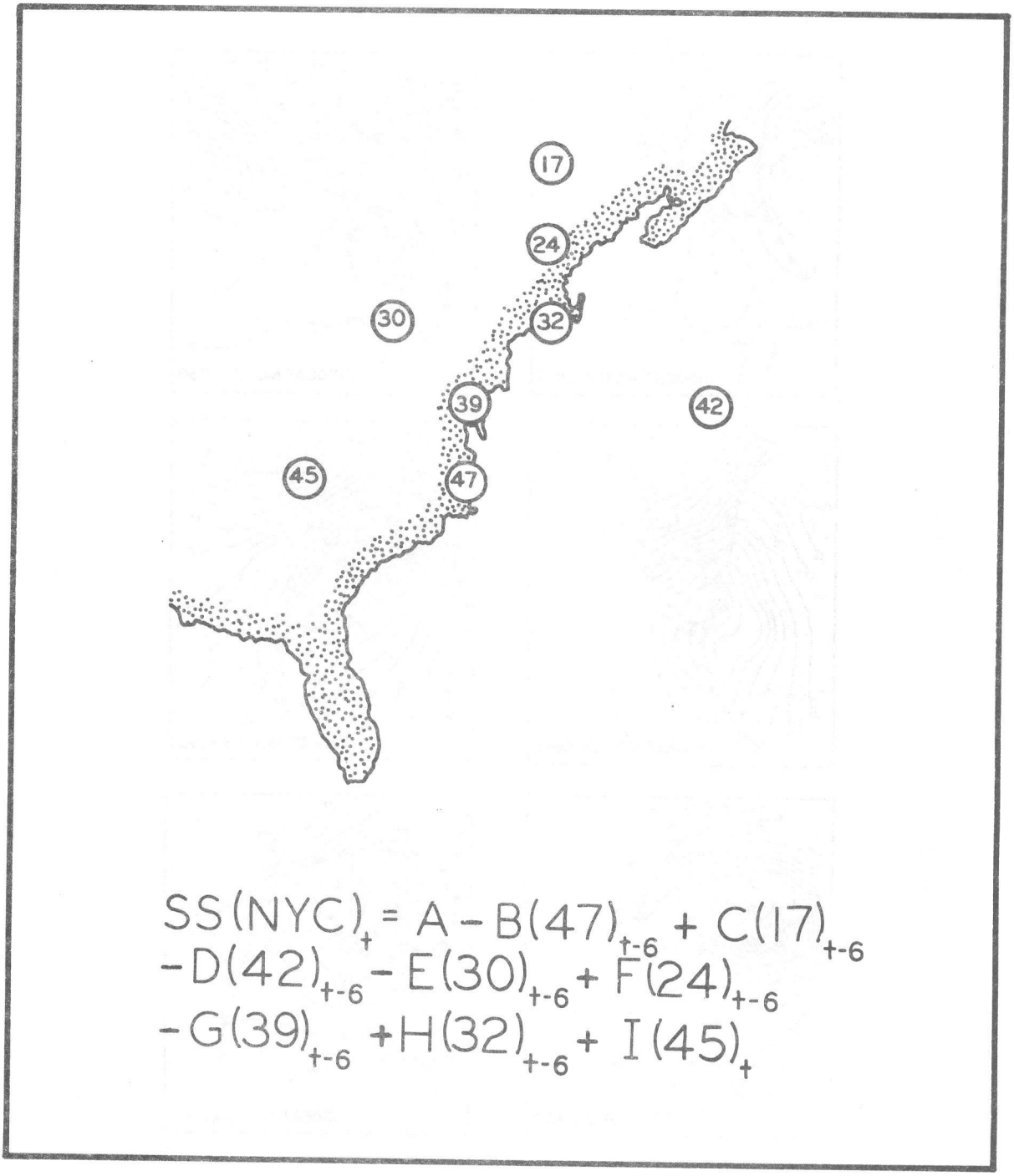

Figure 15. A storm surge forecast equation for New York. SS is the storm surge. The number in parentheses of each term is the grid point for which sea-level pressure is used as a predictor. The subscript on each term is the lag of the predictor in hours.

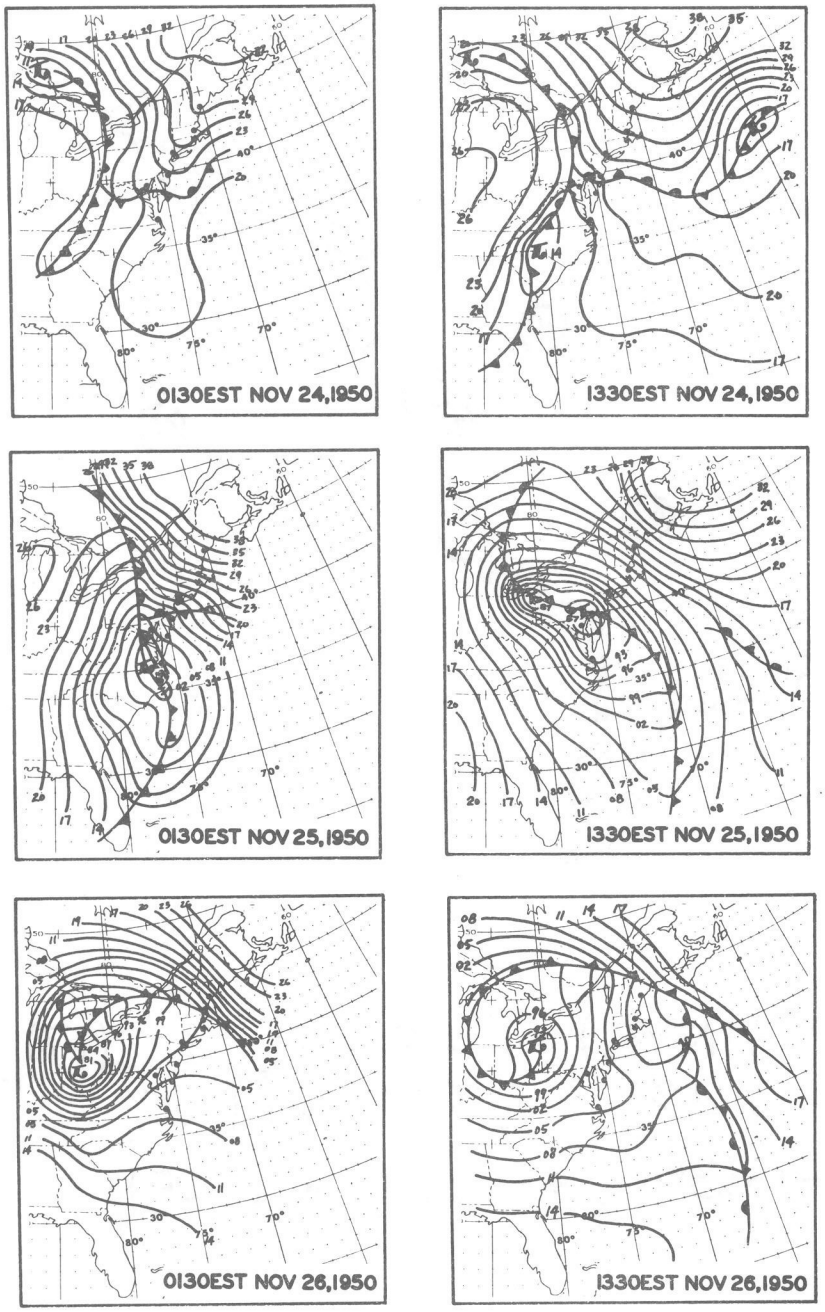

Figure 16. Sea-level pressure charts from 0130EST November 24, 1950 to 1330EST November 26, 1950.

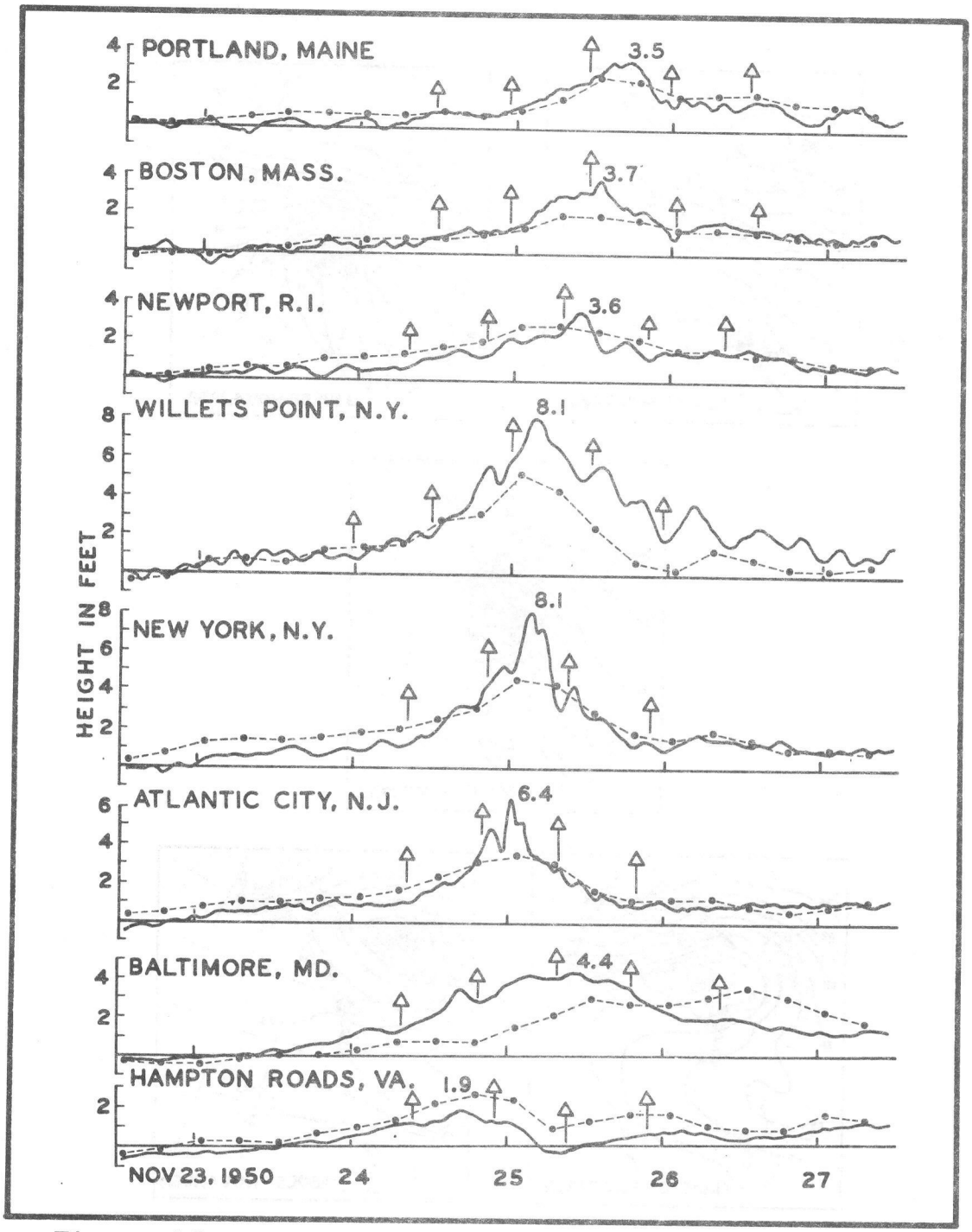

Figure 17. Observed storm surge and computed storm surge for the November 25 - 26, 1950 storm. Solid curves are observed storm surges. Dashed lines join calculated values of surge. Arrows indicate times of astronomical high tides. The date of each day is placed at the 1200EST position. Maximum value of observed surge is placed near peak of each curve.

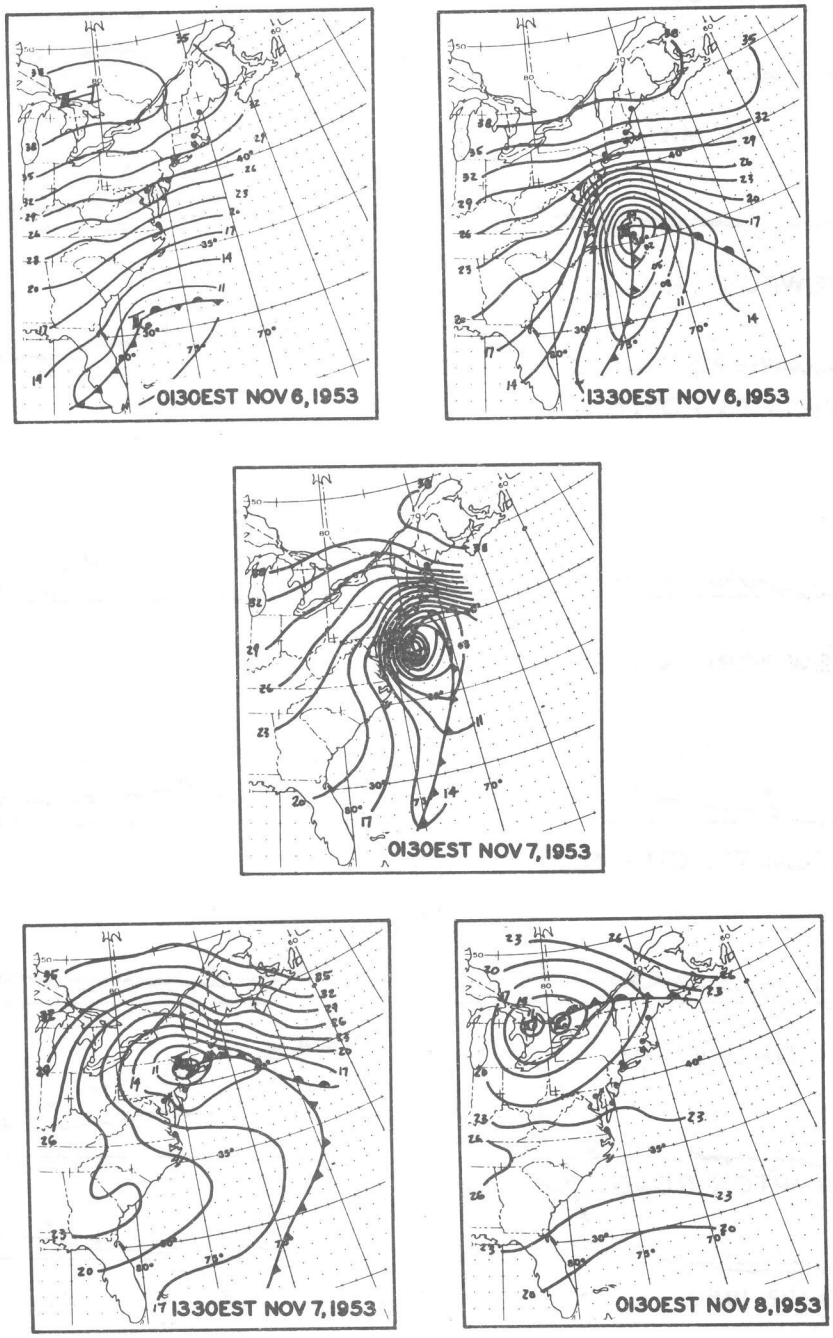

Figure 18. Sea-level pressure charts from 0130EST November 6, 1953 to 0130EST November 8, 1953.

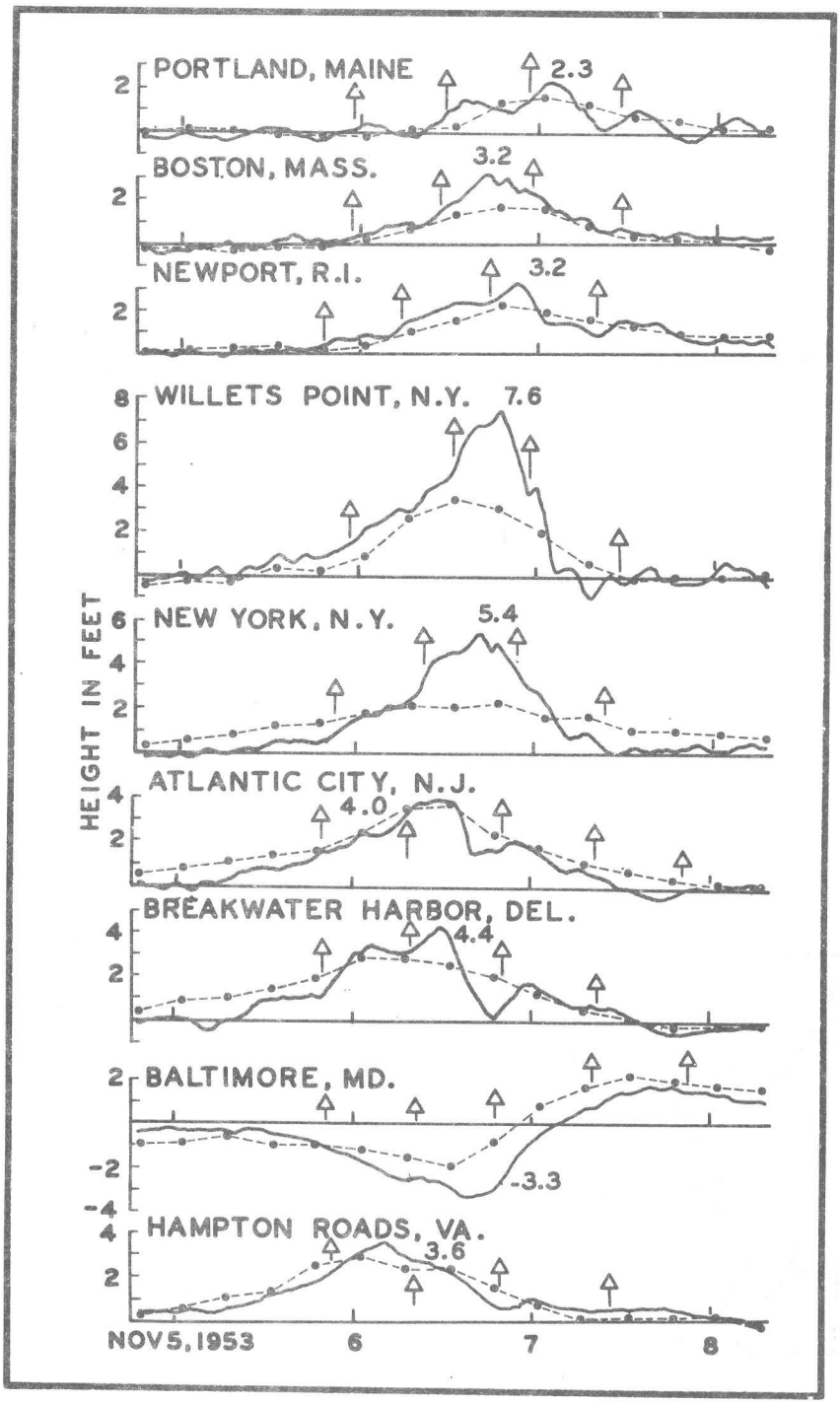

Figure 19. Observed storm surge and computed storm surge for the November 5 - 8, 1953 storm. Solid curves are observed storm surges. Dashed lines join calculated values of surge. Arrows indicate times of astronomical high tides. The date of each day is placed at the 1200EST position. Maximum value of observed surge is placed near peak of each curve.

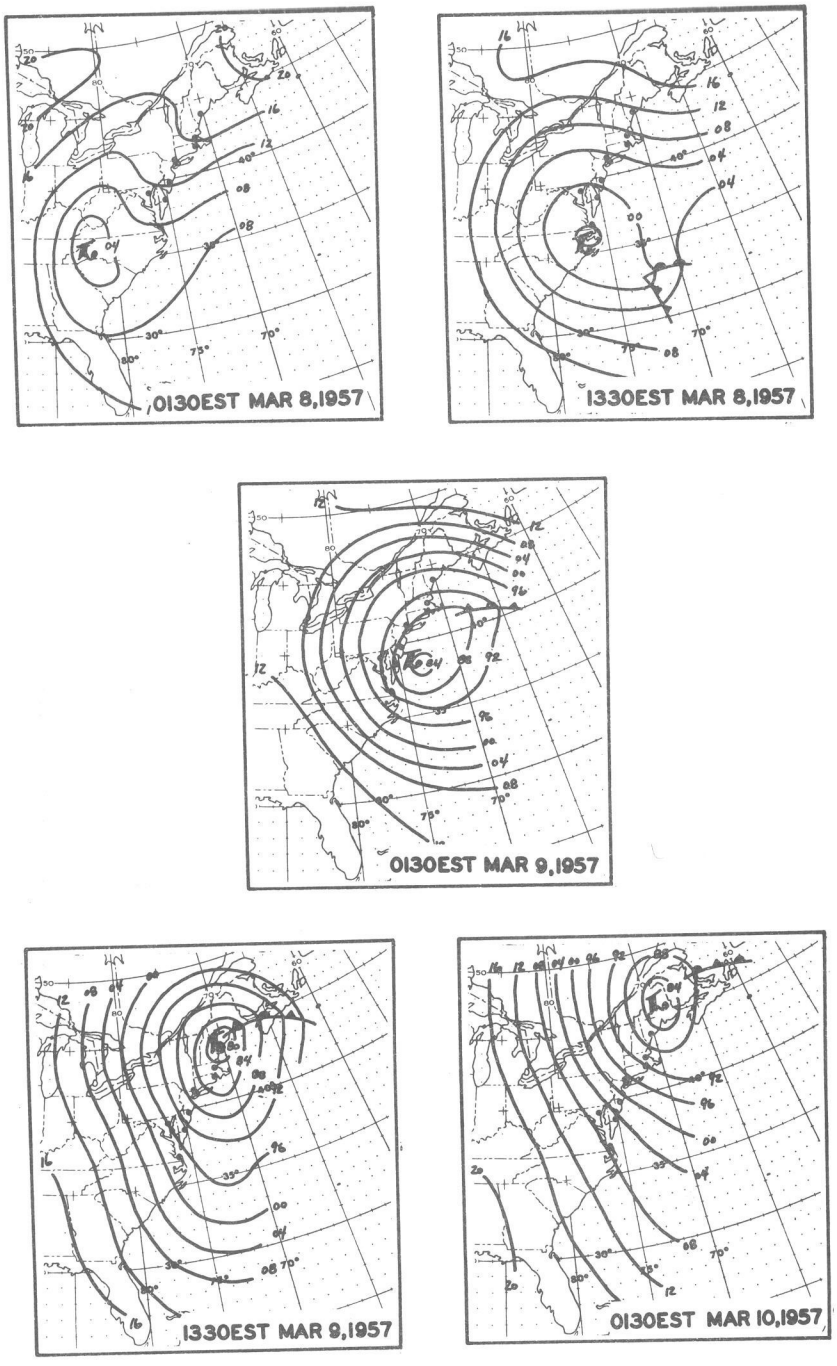

Figure 20. Sea-level pressure charts from 0130EST March 8, 1957 to 0130EST March 10, 1957.

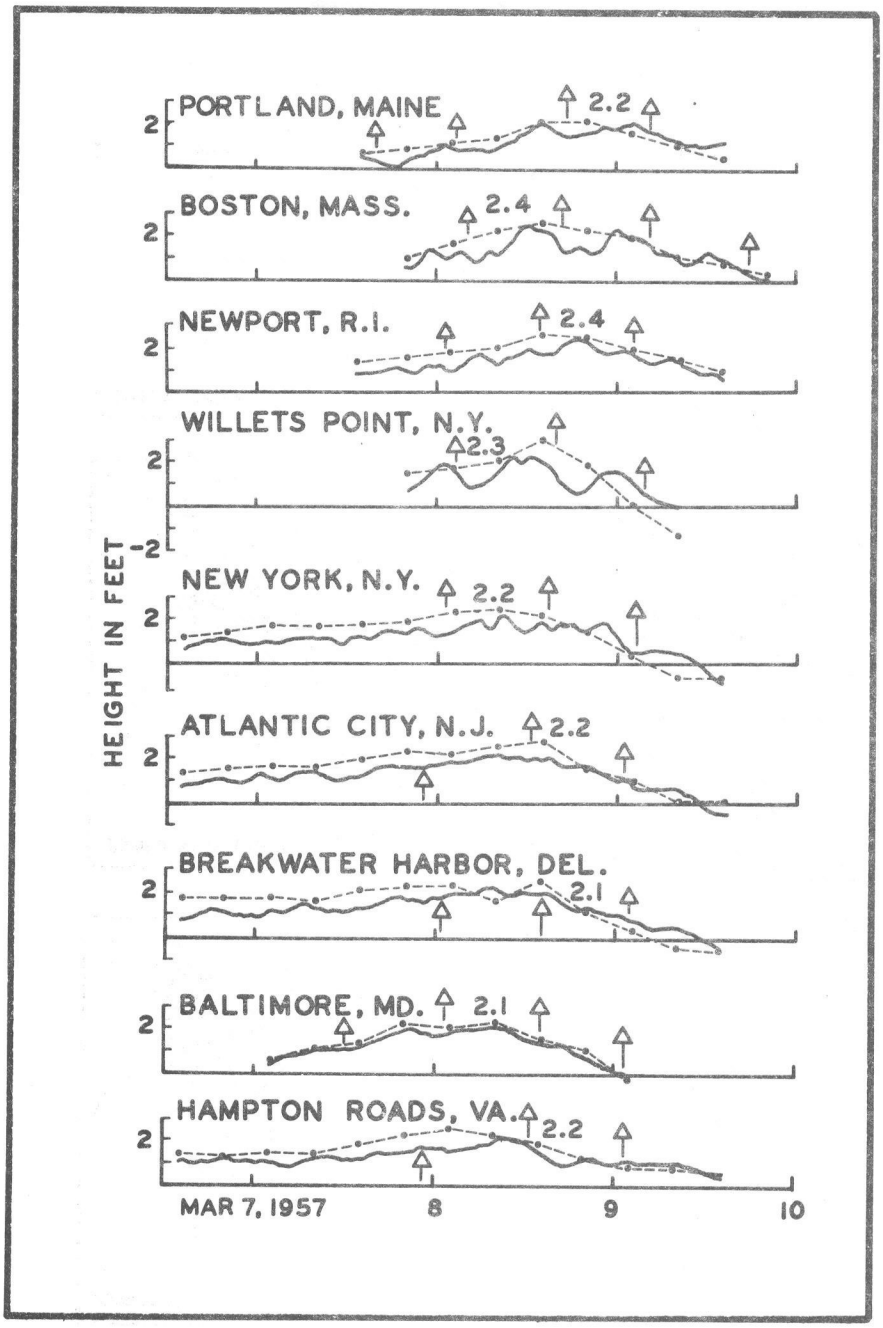

Figure 21. Observed storm surge and computed storm surge for the March 7 - 10, 1957 storm. Solid curves are observed storm surges. Dashed lines join calculated values of surge. Arrows indicate times of astronomical high tide. The date of each day is placed at the 1200EST position. Maximum value of observed surge is placed near peak of each curve.

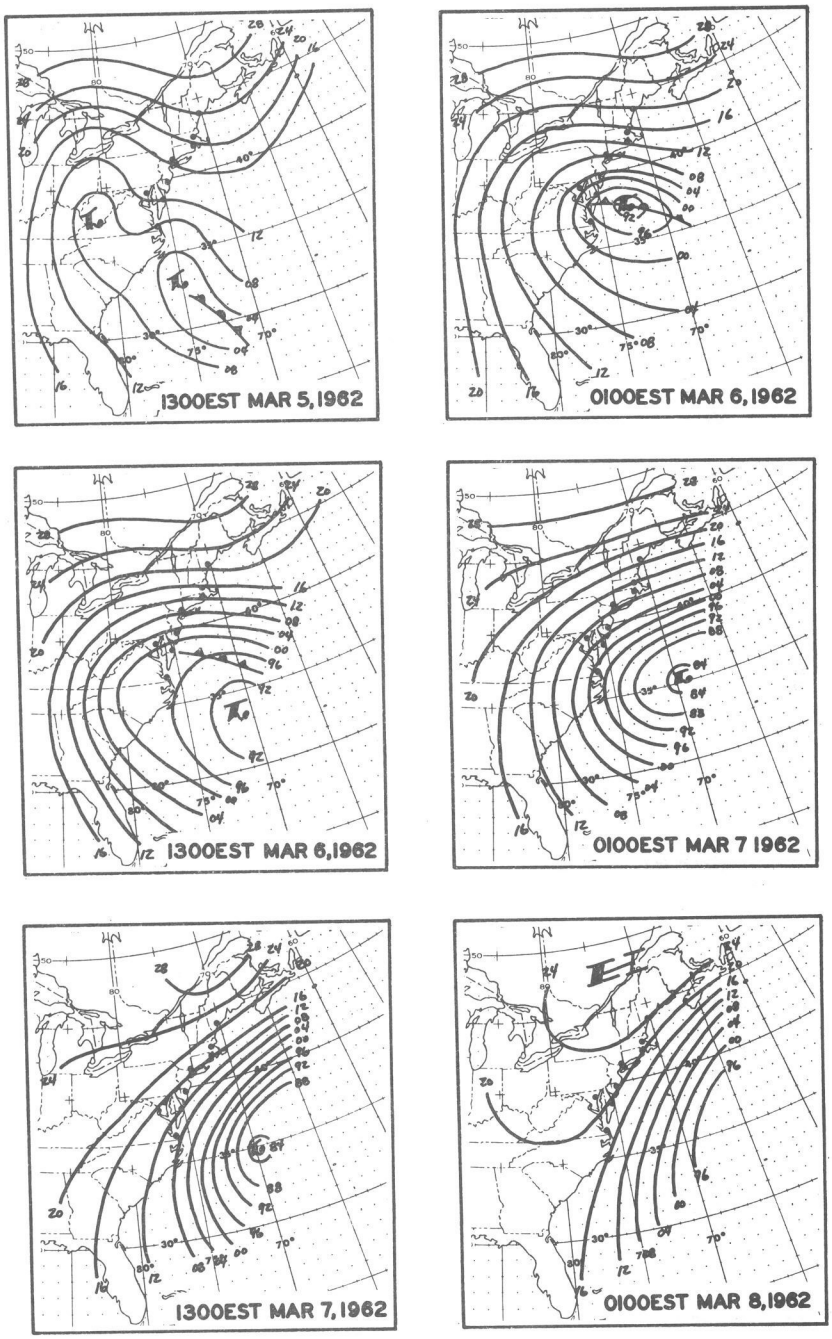

Figure 22. Sea-level pressure charts from 1300EST March 5, 1962 to 0100EST March 8, 1962.

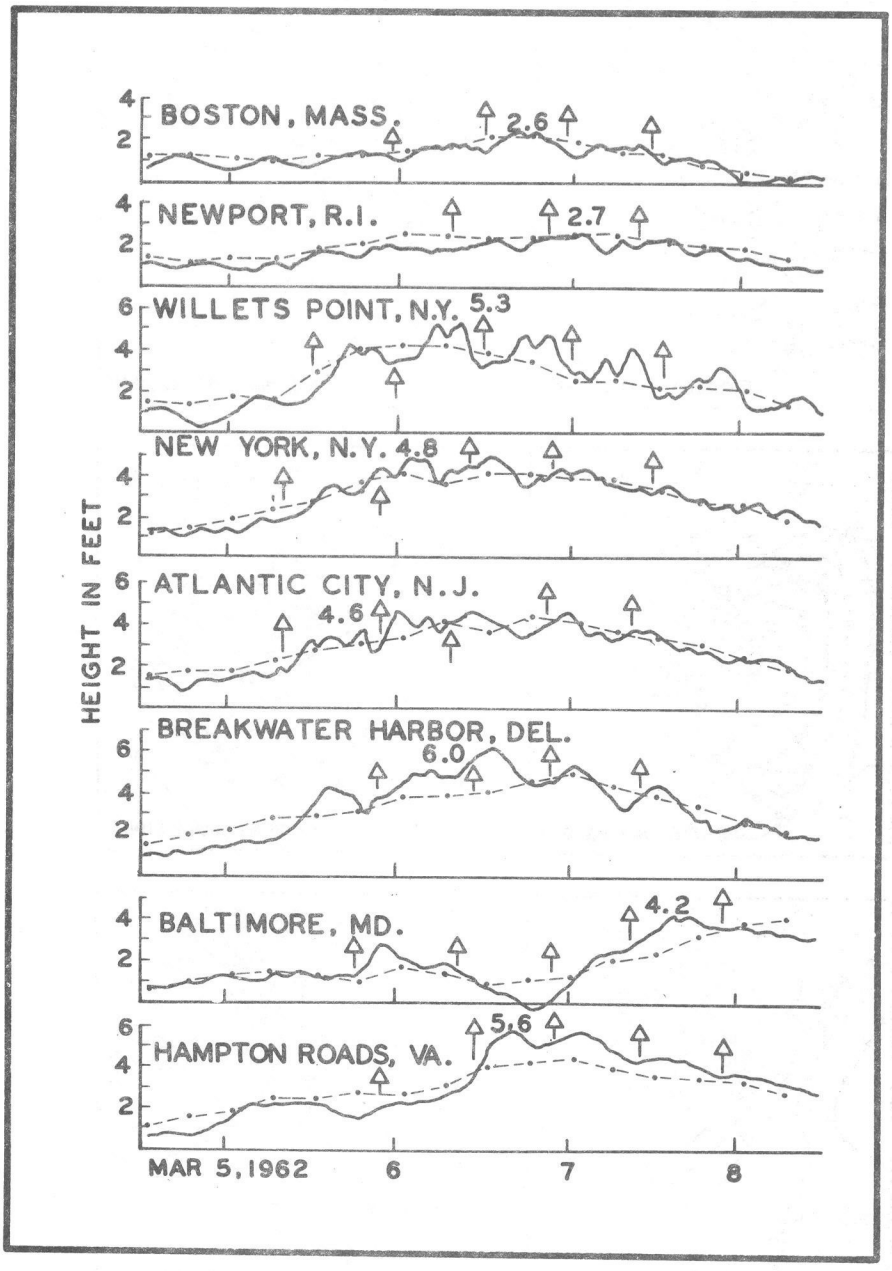

Figure 23. Observed storm surge and computed storm surge for the March 5 - 8, 1962 storm. Solid curves are observed storm surges. Dashed lines join calculated values of surge. Arrows indicate times of astronomical high tides. The date of each day is placed at the 1200EST postion. Maximum value of observed surge is placed near peak of each curve.

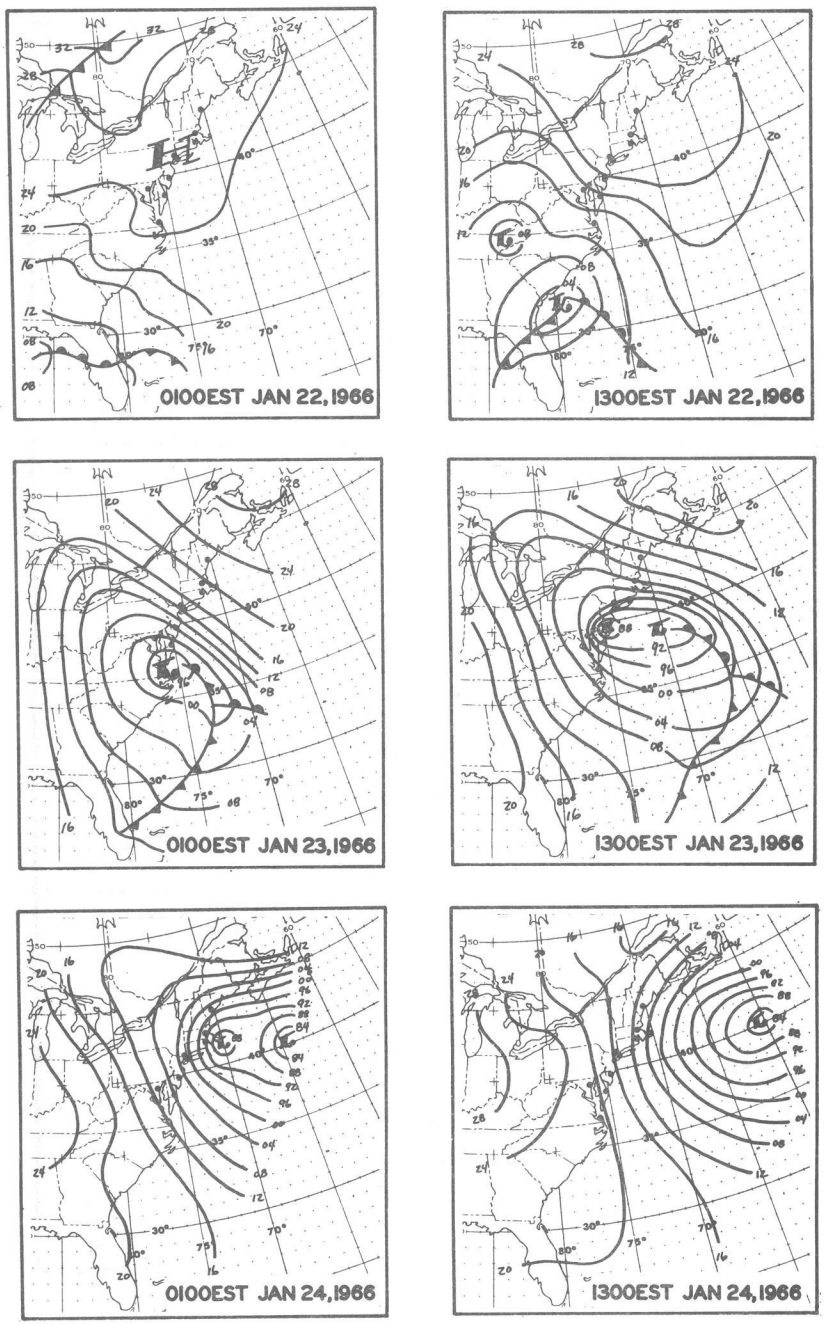

Figure 24. Sea-level pressure charts from 0100EST January 22, 1966 to 1300EST January 24, 1966.

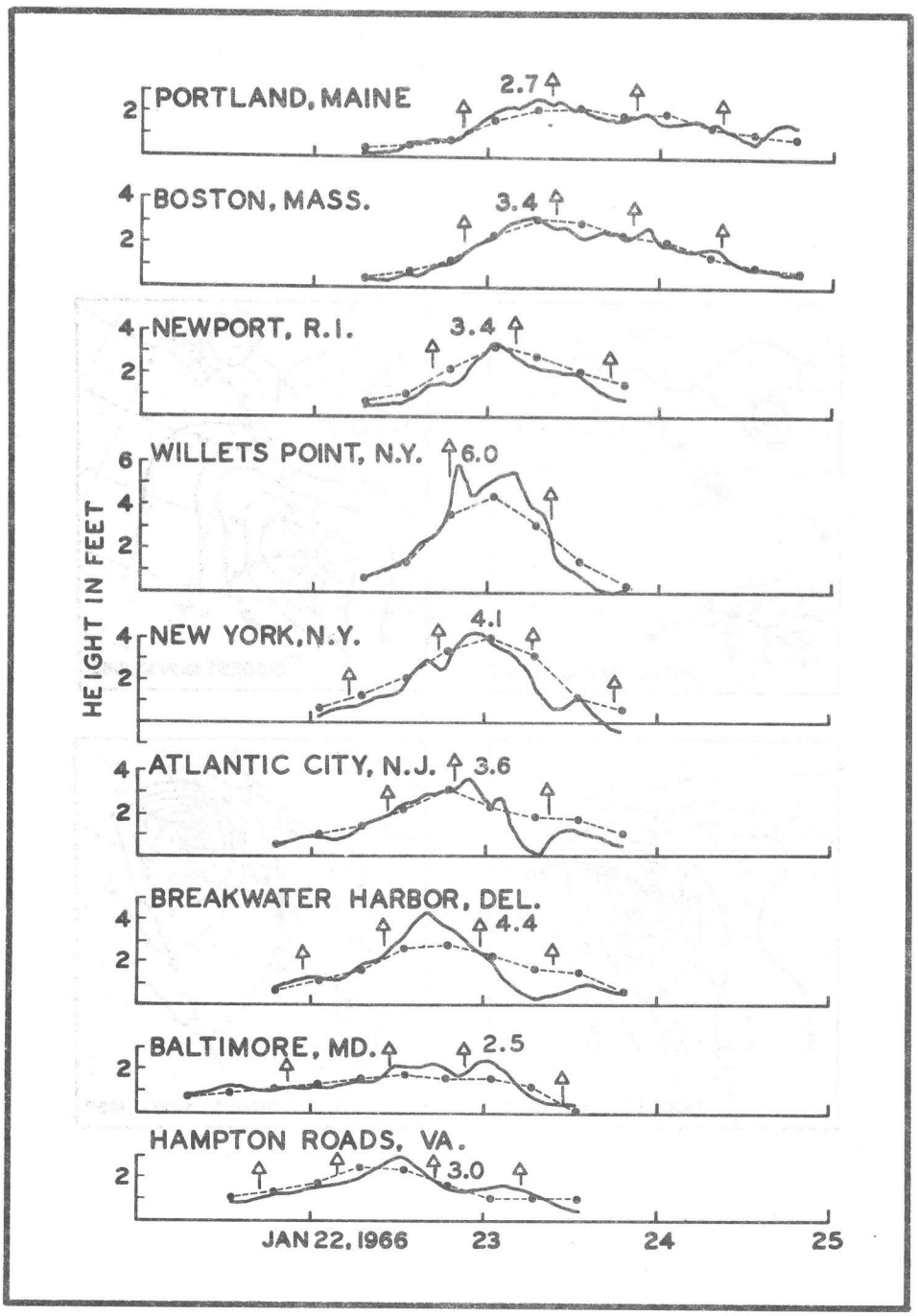

Figure 25. Observed storm surge and computed storm surge for the January 22 - 25, 1966 storm. Solid curves are observed storm surges. Dashed lines join calculated values of surge. Arrows indicate times of astronomical high tides. The date of each day is placed at the 1200EST position. Maximum value of observed surge is placed near peak of each curve.

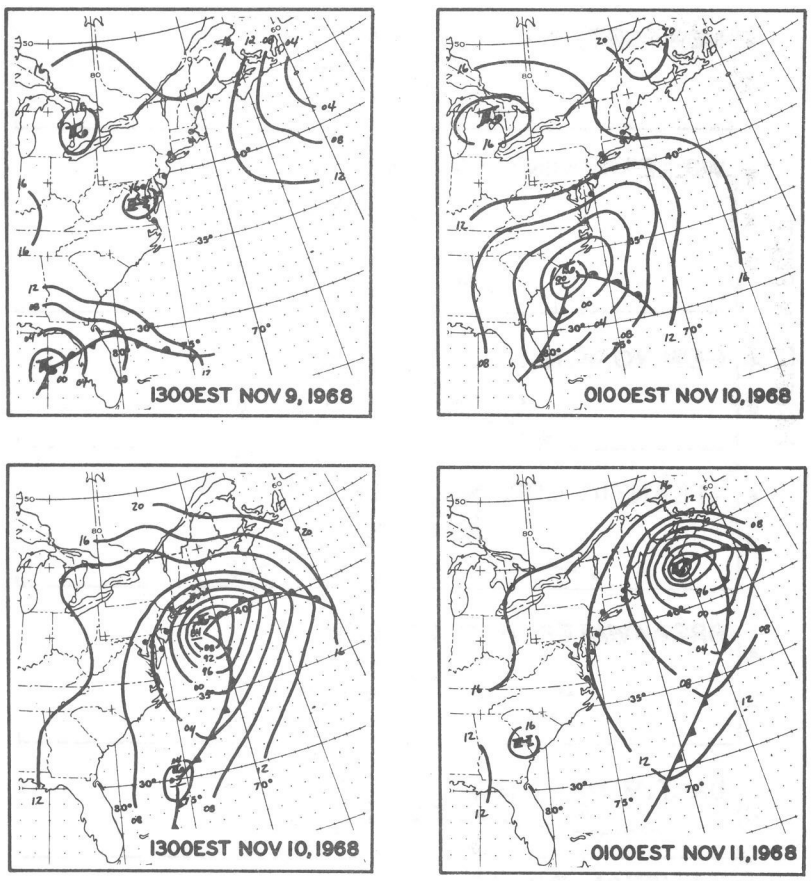

Figure 26. Sea-level pressure charts from 1300EST November 9, 1968 to 0100EST November 11, 1968.

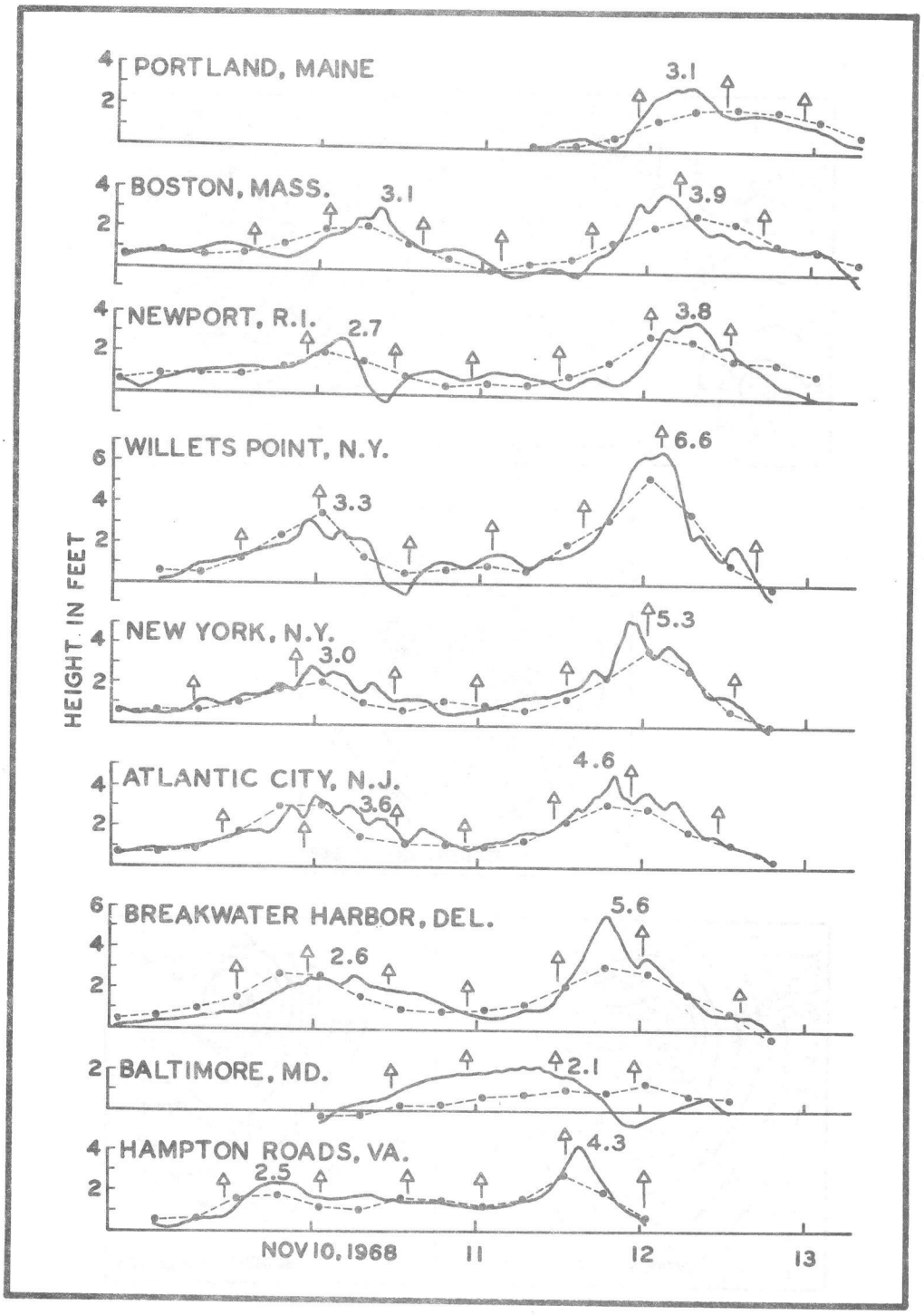

Figure 27. Observed storm surge and computed storm surge for the November 10 - 13, 1968 storms. Solid curves are observed storm surges. Dashed lines join calculated values of surge. Arrows indicate times of astronomical high tides. The date of each day is placed at the 1200EST position. Maximum value of observed surge is placed near peak of each curve.

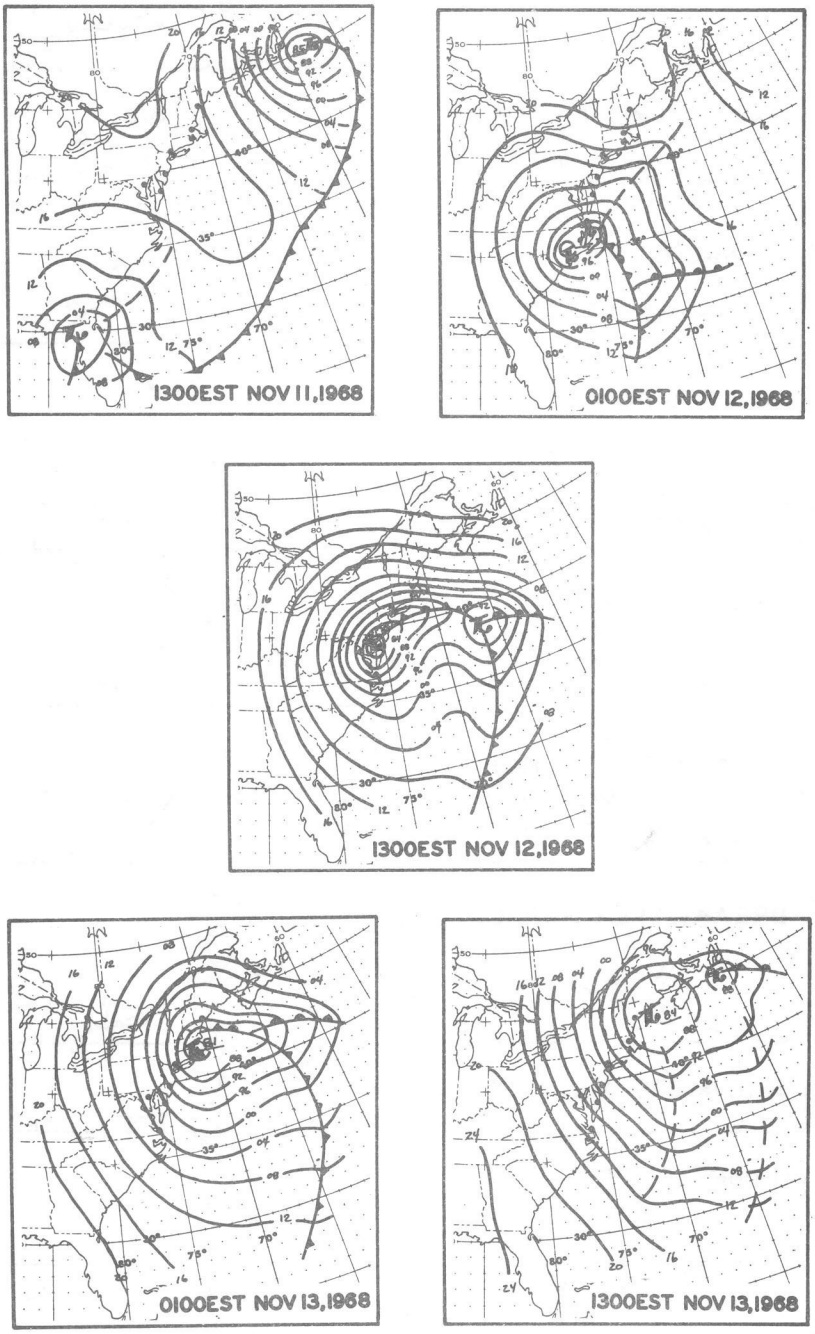

Figure 28. Sea-level pressure charts from 1300EST November 11, 1968 to 1300EST November 13, 1968.

FZUS3 KWBC 021200
STORM SURGE FCST FEET INVALID FOR TROPICAL STORMS

	12Z	18Z	00Z	06Z	12Z	18Z	00Z	06Z	12Z
PWM	0.1	0.4	0.5	0.7	0.7	0.9	0.8	0.9	0.7
BOS	0.1	0.2	0.3	0.4	0.4	0.5	0.4	0.6	0.3
NWP	0.8	1.0	1.1	1.2	1.2	1.3	1.1	1.1	0.9
SFD	1.0	1.1	1.2	1.2	0.9	0.7	0.6	0.1	0.0
LGA	1.0	1.0	1.0	1.3	1.2	1.0	1.0	0.8	0.7
NYC	1.2	1.3	1.4	1.4	1.3	1.2	1.0	0.9	0.7
ACY	0.8	0.9	1.0	0.9	0.9	0.9	0.8	0.8	0.7
BWH	1.1	1.1	1.2	1.0	0.9	0.9	0.7	0.7	0.6
BAL	2.4	2.5	2.6	2.8	2.8	2.6	2.4	2.0	1.9
ORF	0.9	0.8	0.9	0.8	0.8	0.8	0.7	0.6	0.9

PWM Portland, Maine
BOS Boston, Massachusetts
NWP Newport, Rhode Island
SFD Stamford, Connecticut
LGA Willets Point, New York
NYC New York, New York
ACY Atlantic City, New Jersey
BWH Breakwater Harbor, Delaware
BAL Baltimore, Maryland
ORF Hampton Roads, Virginia

Figure 29. Storm surge forecast teletype message. Forecast heights are in feet. Valid times are indicated above each column of heights. Station call signs are identified below the message.

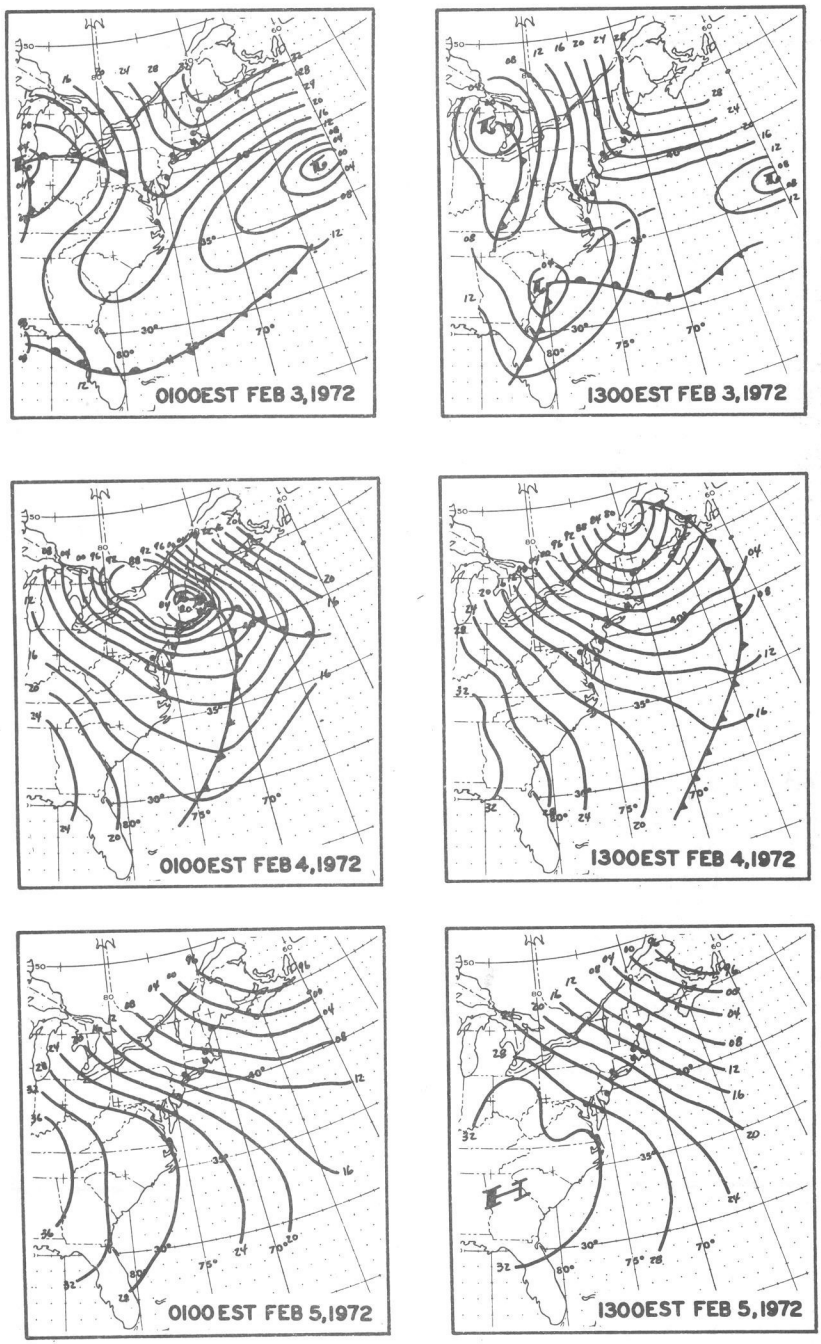

Figure 30. Sea-level pressure charts from 0100EST February 3, 1972 to 1300EST February 5, 1972.

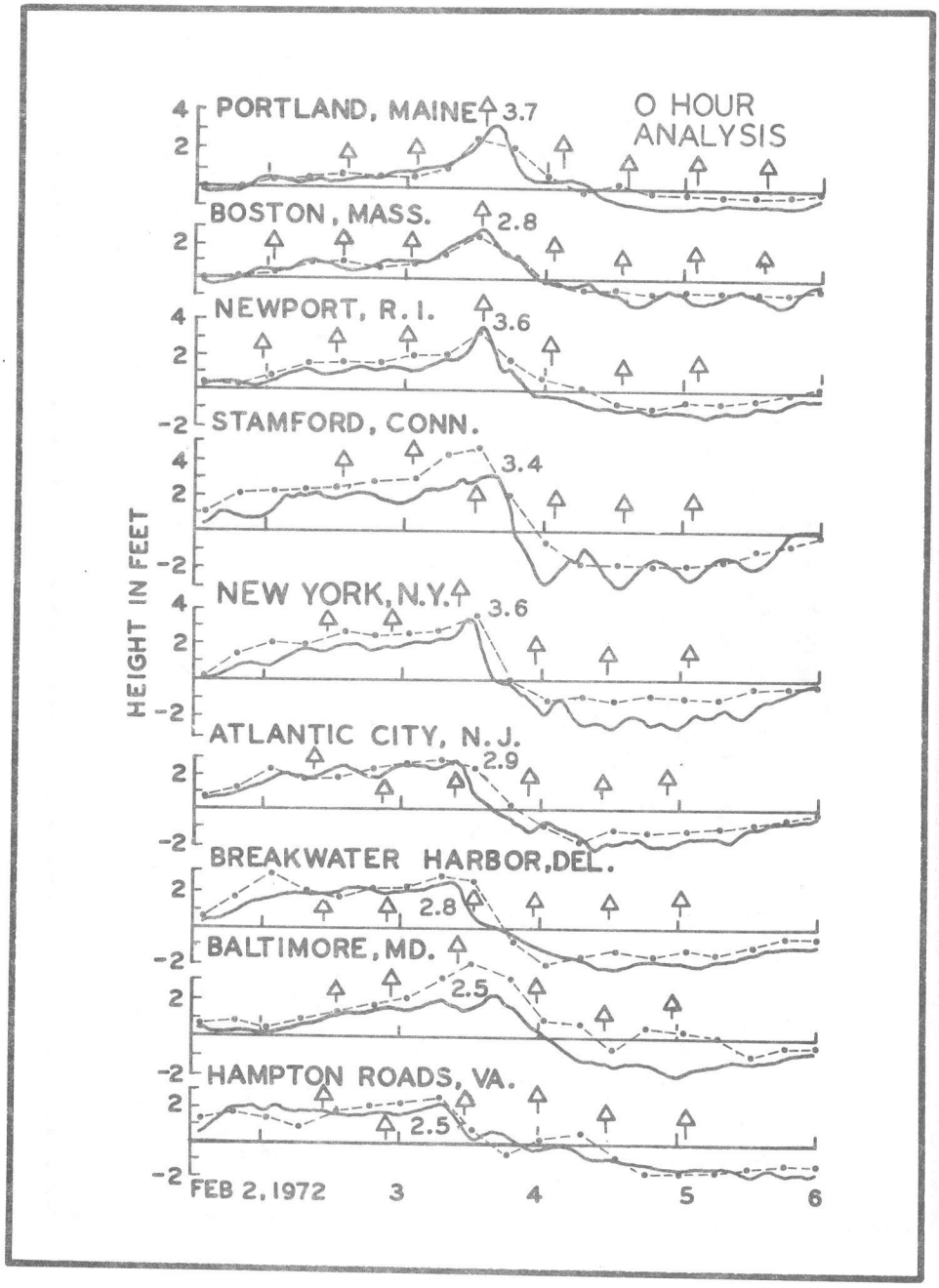

Figure 31. Storm surge calculations based on sea-level pressure analyses are shown by dots. Solid curves indicate observed storm surges. Arrows indicate times of astronomical high tide. The date for each day is placed at the 1200EST position. Maximum value of observed surge is placed near peak of each curve.

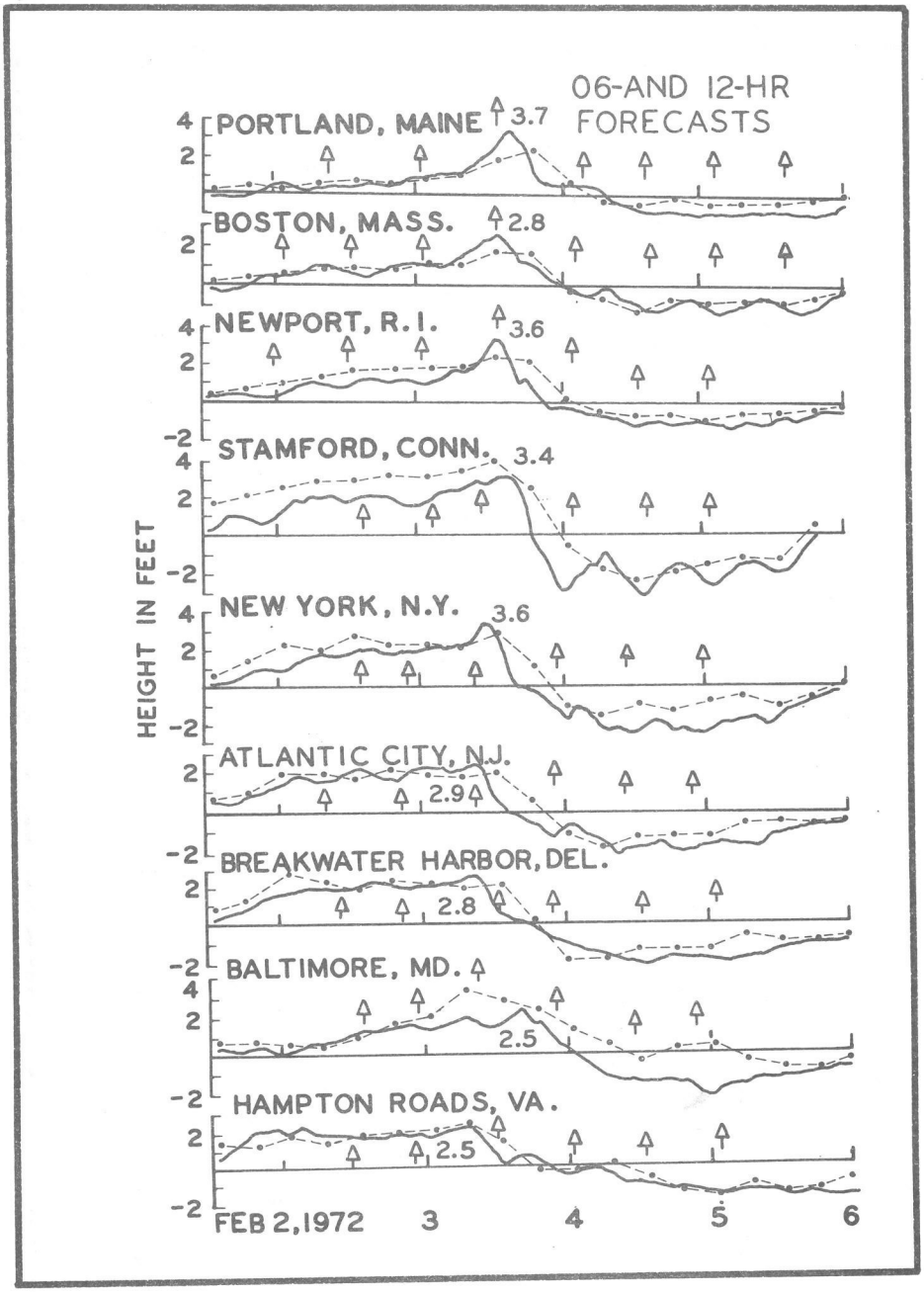

Figure 32. Six- and 12-hour forecasts of storm surge based on sea-level pressure forecasts of the PE model are shown by dots. Solid curves indicate observed storm surges. Arrows indicate times of astronomical high tide. The date for each day is placed at the 1200 EST position. Maximum value of observed surge is placed near peak of each curve.

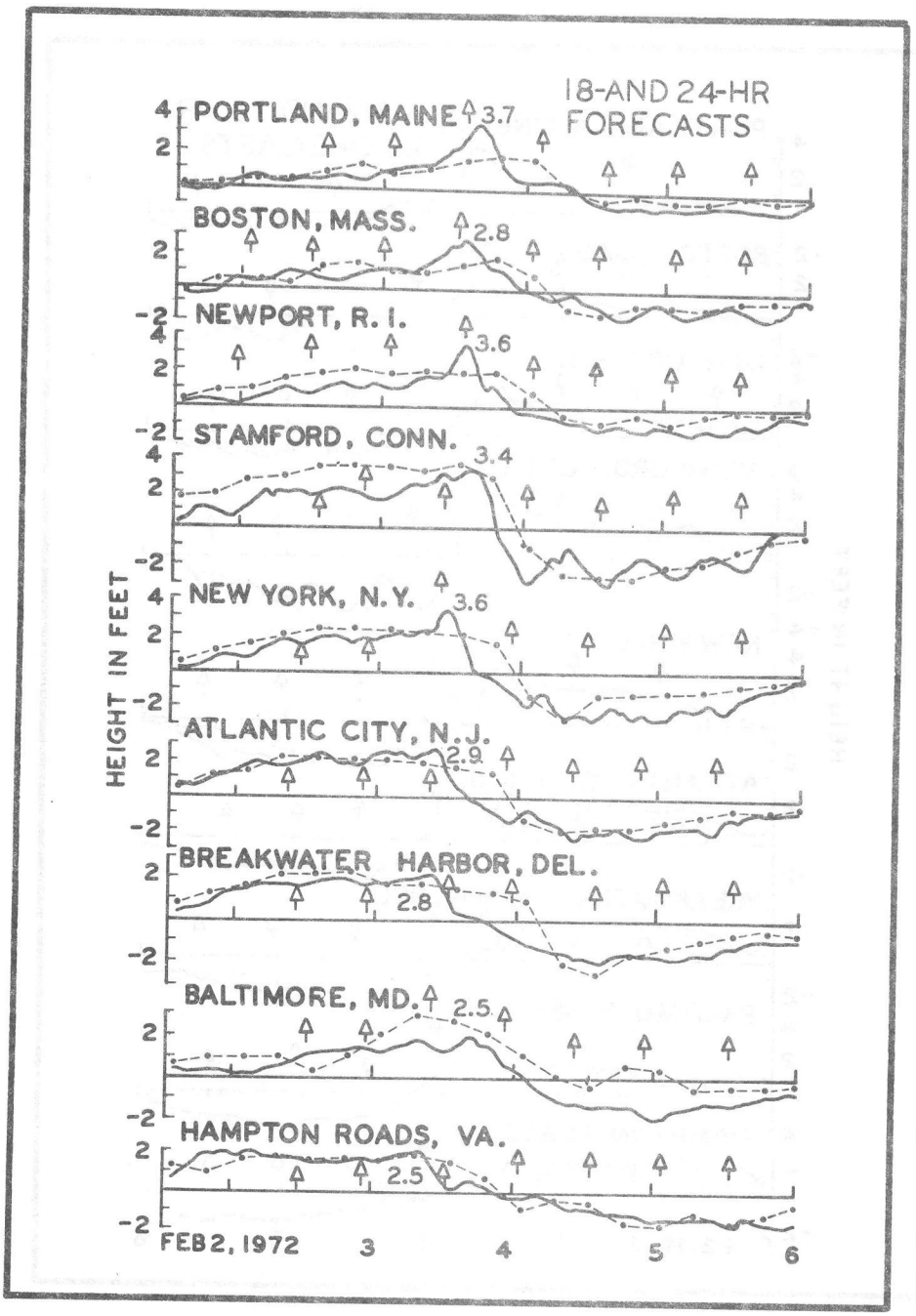

Figure 33. Eighteen- and 24-hour forecasts of storm surge based on sea-level pressure forecasts of the PE model are shown by dots. Solid curves indicate observed storm surges. Arrows indicate times of astronomical high tide. The date for each day is placed at the 1200 EST position. Maximum value of observed surge is placed near peak of each curve.

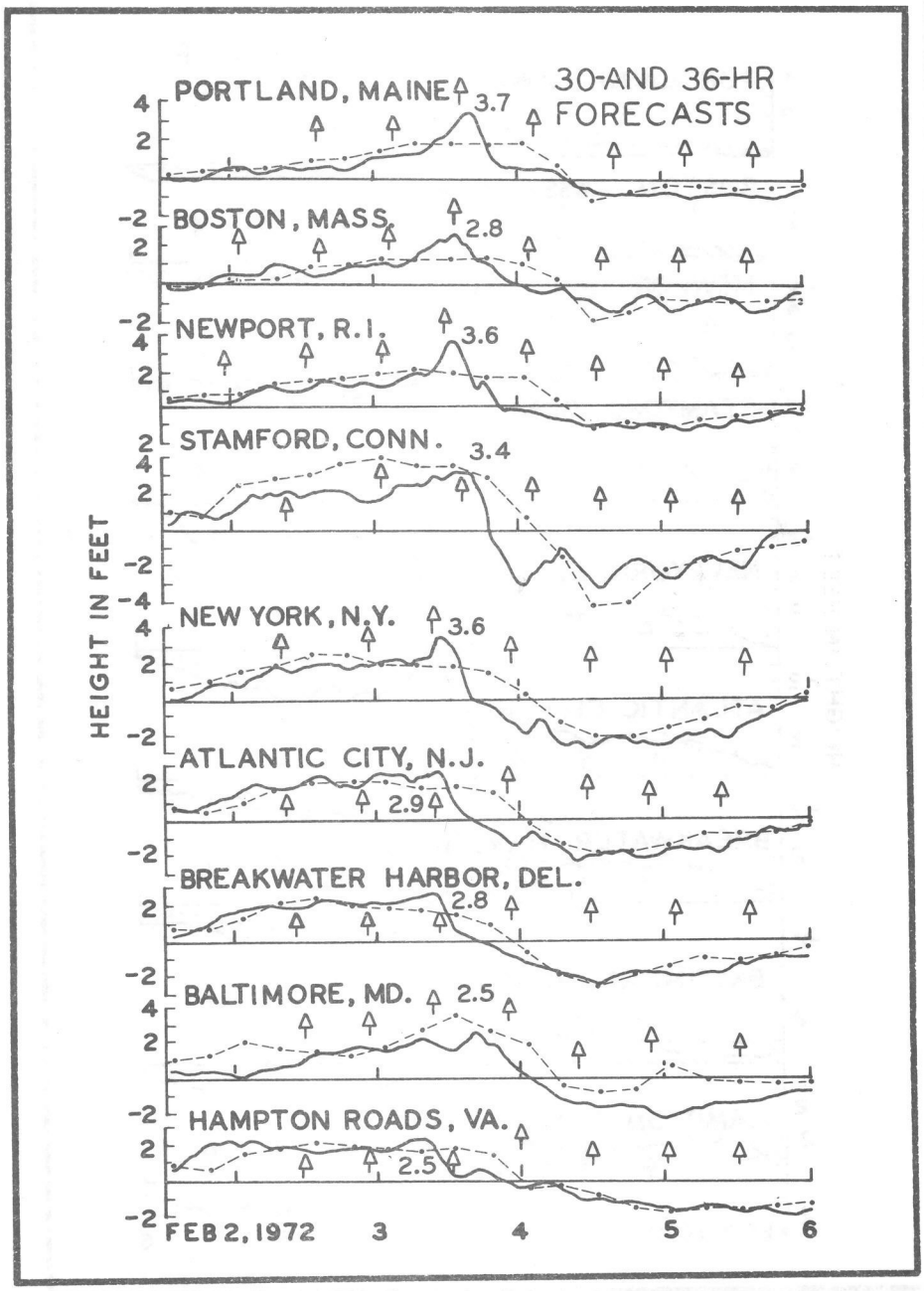

Figure 34. Thirty- and 36-hour forecasts of storm surge based on sea-level pressure forecasts of the PE model are shown by dots. Solid curves indicate observed storm surges. Arrows indicate times of astronomical high tide. The date for each day is placed at the 1200 EST position. Maximum value of observed surge is placed near peak of each curve.

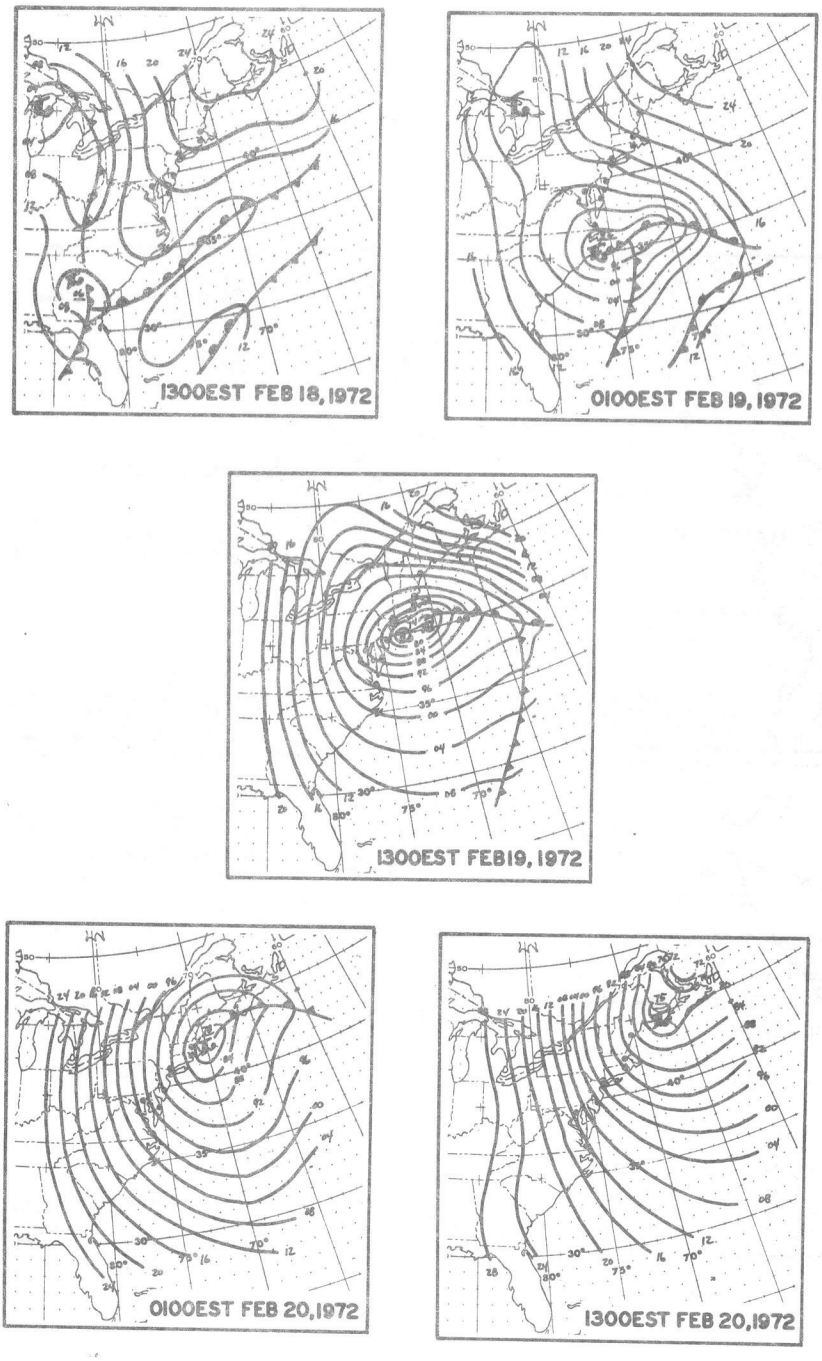

Figure 35. Sea-level pressure charts from 1300EST February 18, 1972 to 1300EST February 20, 1972.

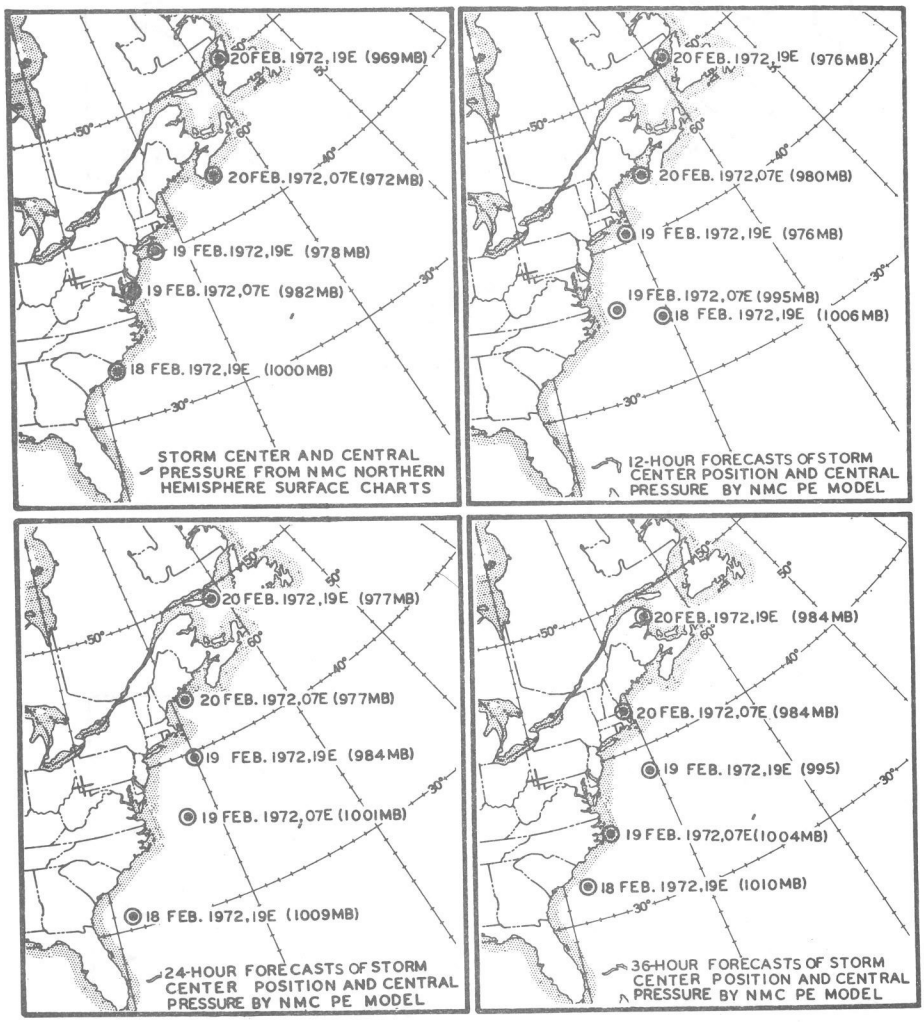

Figure 36. Analyzed and forecast values of storm center position and central pressure. Data taken from NMC analyzed surface pressure charts and grid point values of sea-level pressure forecasts of the PE model.

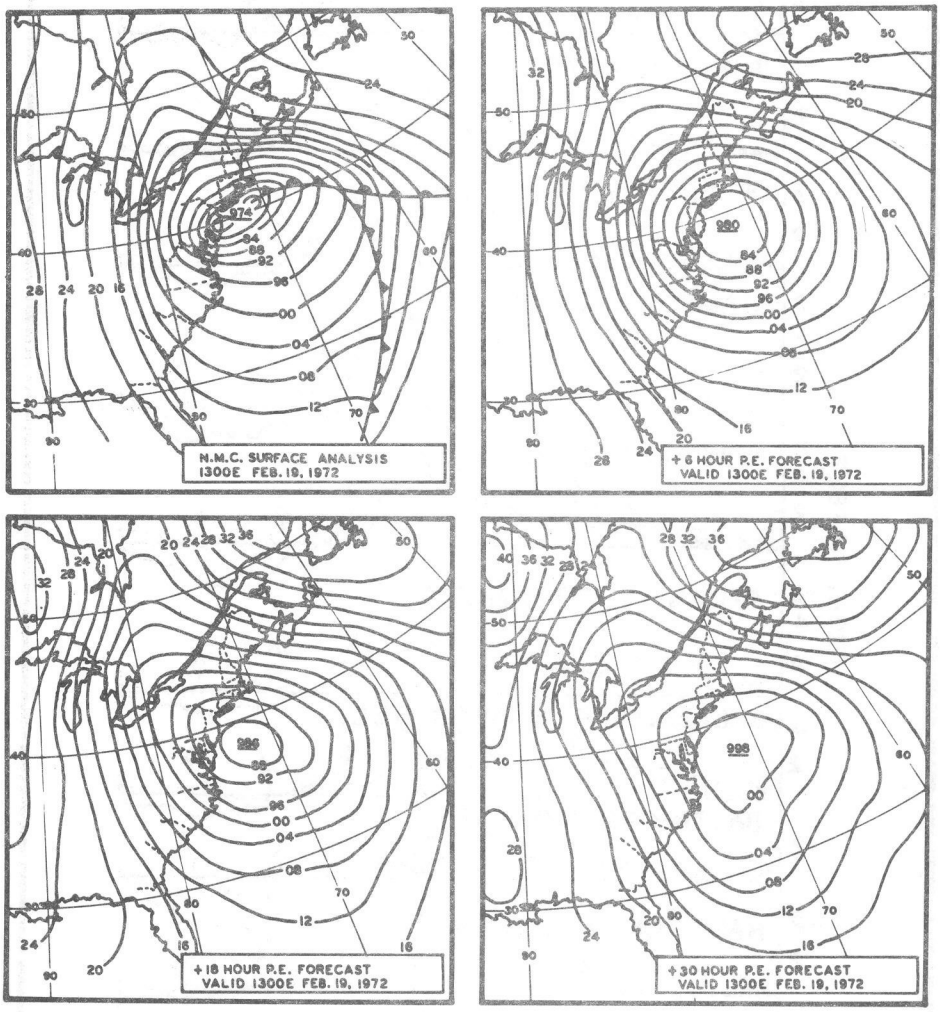

Figure 37. Sea-level pressure analysis for 1300EST on February 19, 1972 and the 6-hour, 18-hour and 30-hour forecasts by the PE model of the National Meteorological Center.

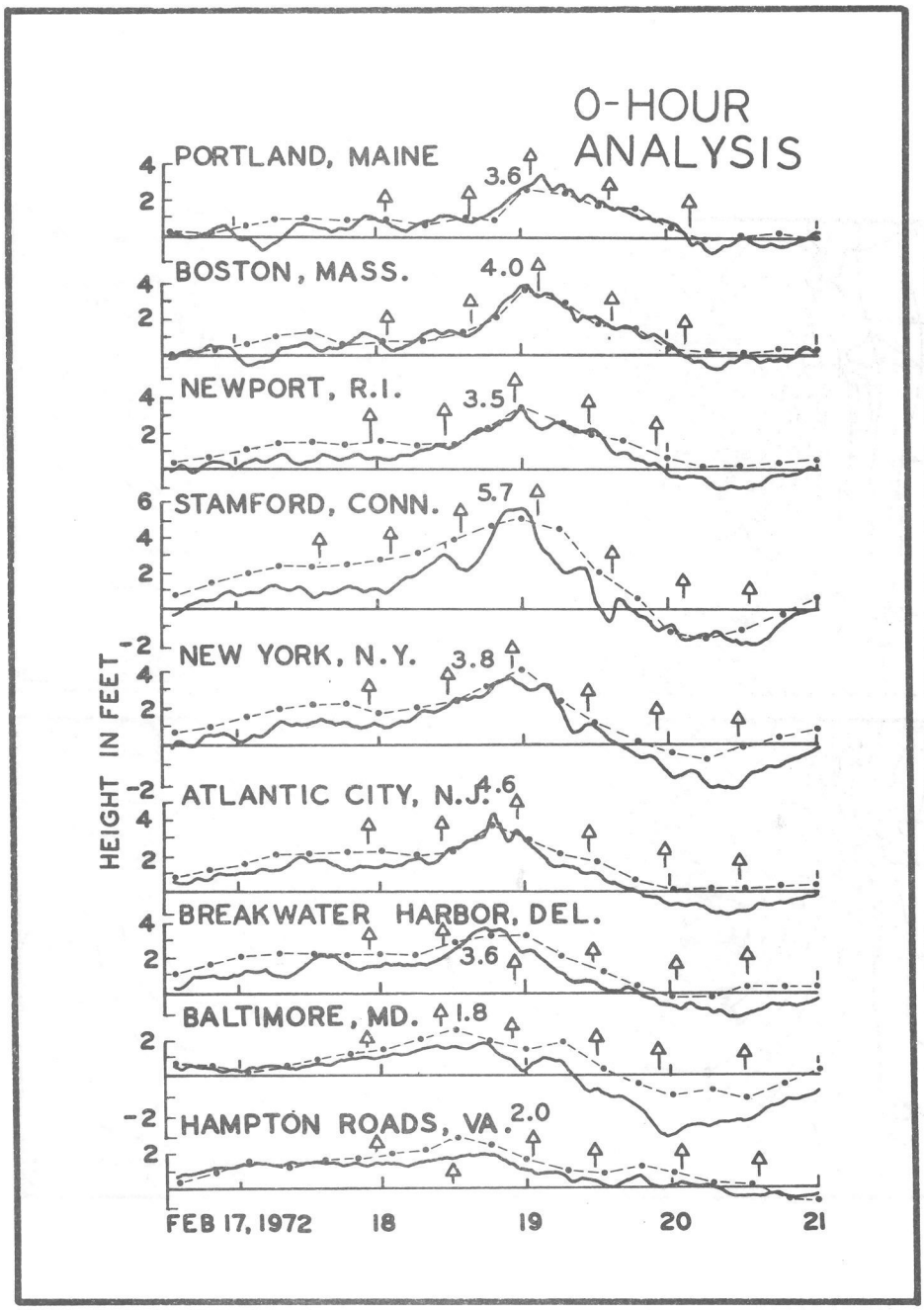

Figure 38. Storm surge calculations based on sea-level pressure analyses are shown by dots. Solid curves indicate observed storm surges. Arrows indicate times of astronomical high tide. The date for each day is placed at the 1200EST position. Maximum value of observed surge is placed near peak of each curve.

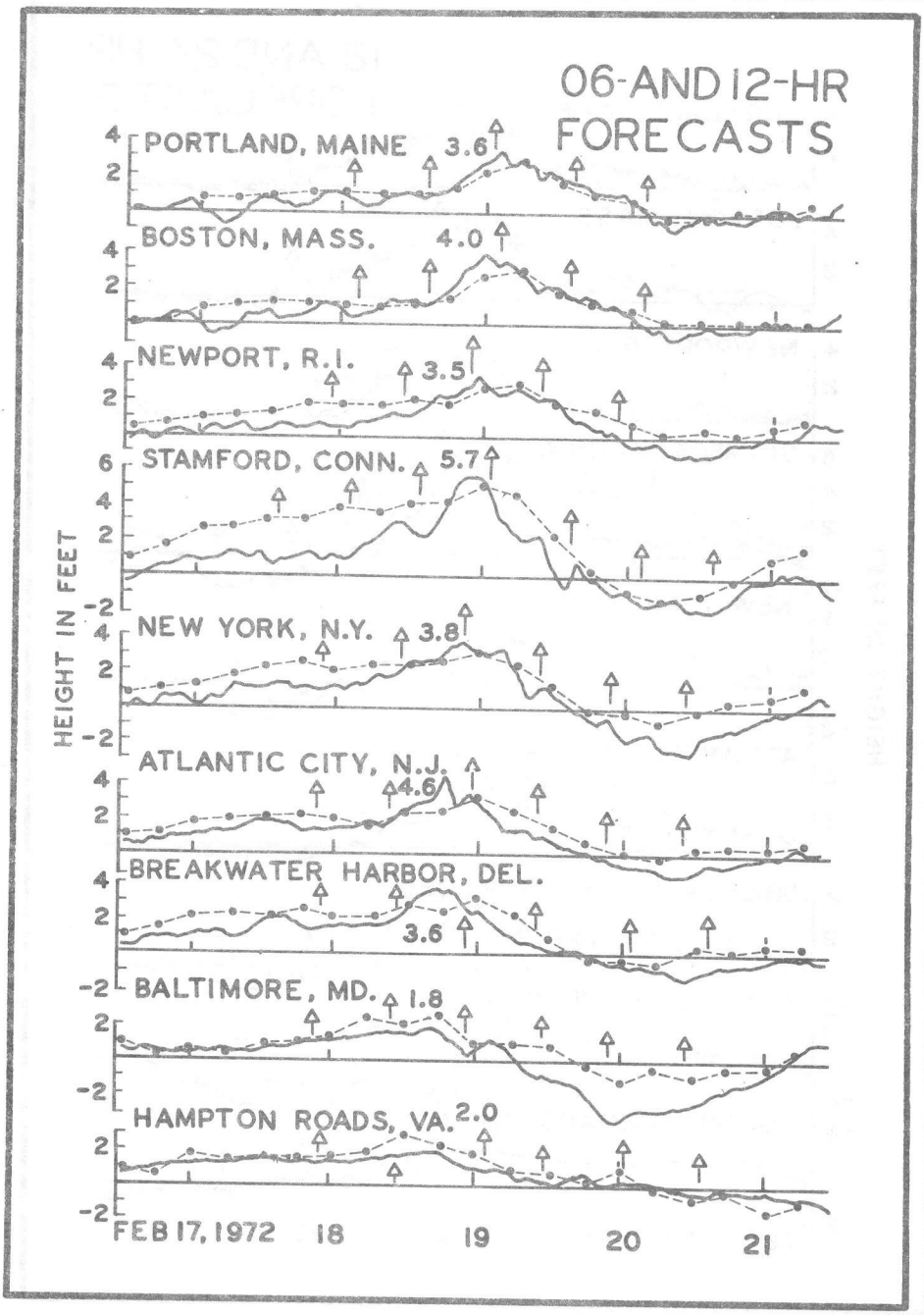

Figure 39. Six- and 12-hour forecasts of storm surge based on sea-level pressure forecasts of the PE model are shown by dots. Solid curves indicate observed storm surges. Arrows indicate times of astronomical high tide. The date of each day is placed at the 1200 EST position. Maximum value of observed surge is placed near peak of each curve.

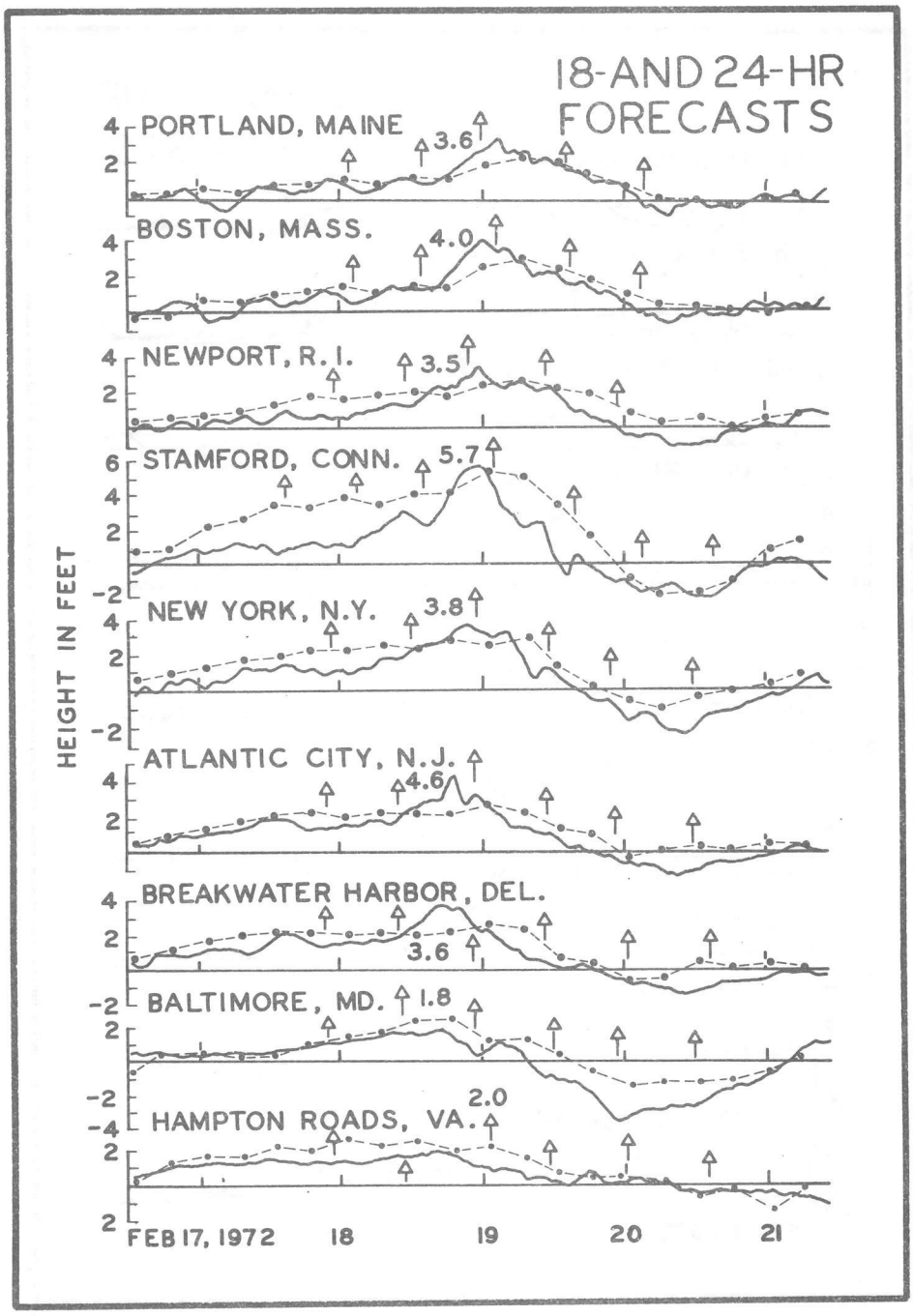

Figure 40. Eighteen- and 24-hour forecasts of storm surge based on sea-level pressure forecasts of the PE model are shown by dots. Solid curves indicate observed storm surges. Arrows indicate times of astronomical high tide. The date of each day is placed at the 1200 EST position. Maximum value of observed surge is placed near peak of each curve.

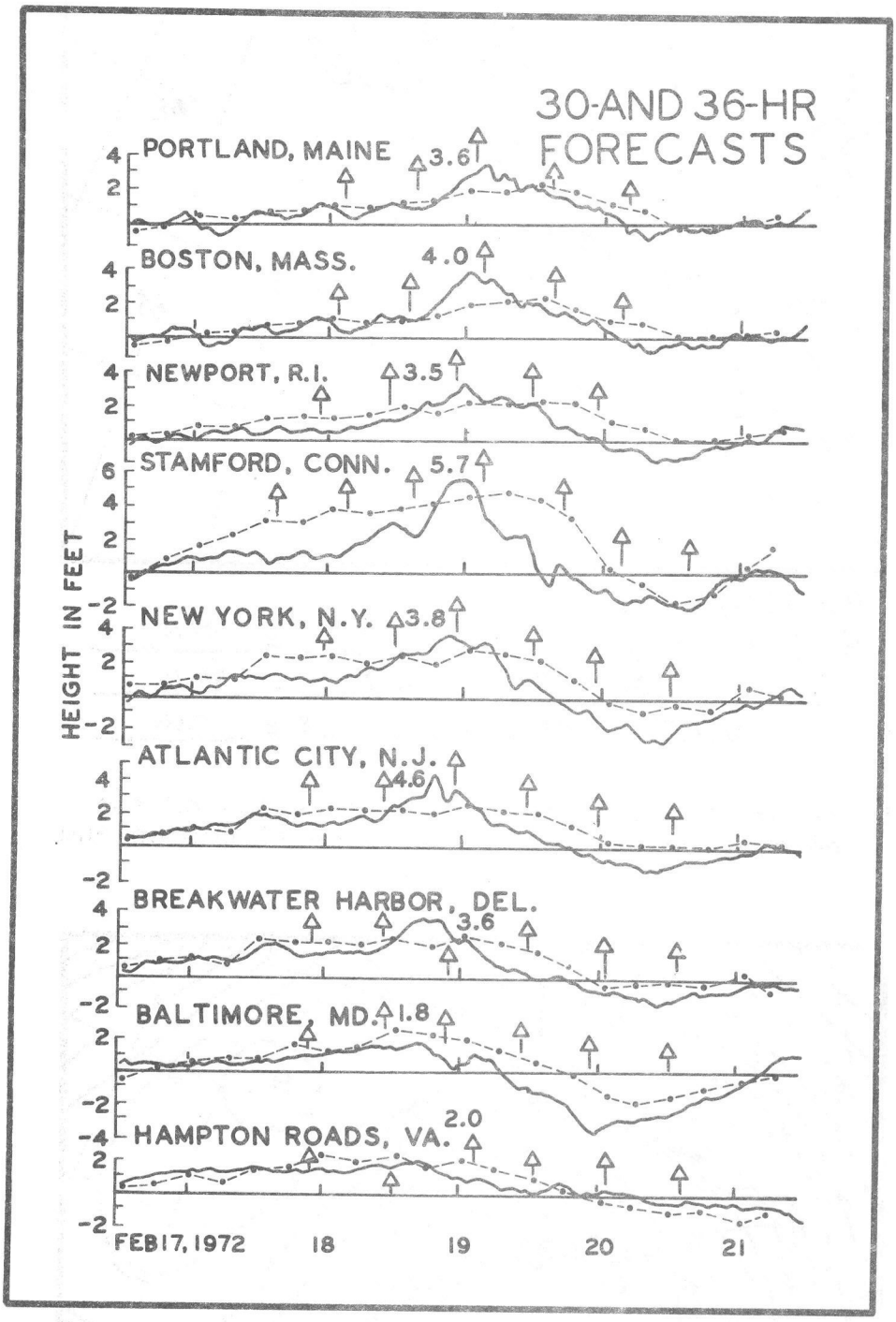

Figure 41. Thirty- and 36-hour forecasts of storm surge based on sea-level pressure forecasts of the PE model are shown by dots. Solid curves indicate observed storm surges. Arrows indicate times of astronomical high tide. The date of each day is placed at the 1200 EST position. Maximum value of observed surge is placed near peak of each curve.

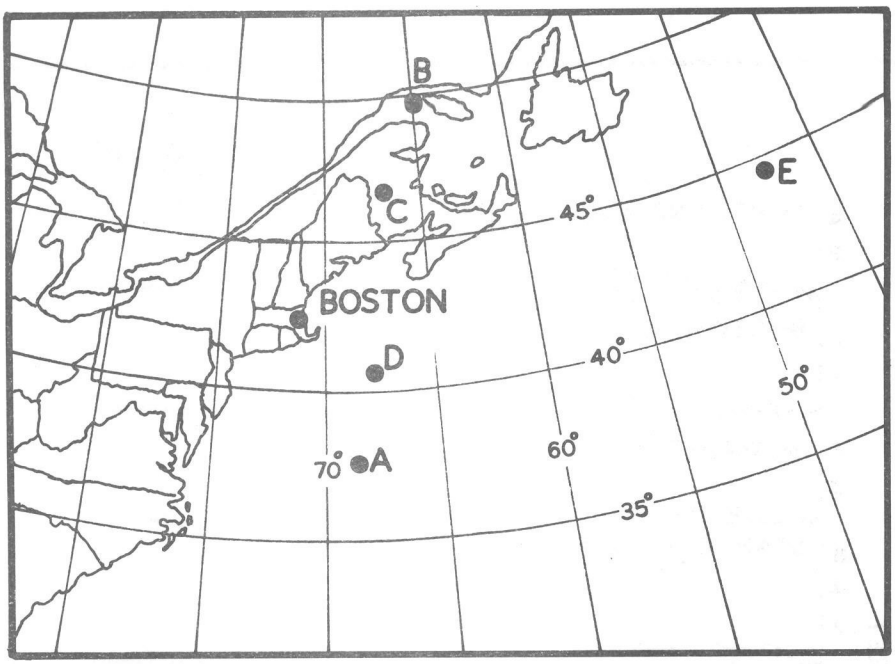

BOSTON, MASS.

(A') 41.55 + (B') 25.10 + (C') 30.51 = 97.16

(D') -83.14 + (E') -10.96 = -94.10

STORM SURGE FORECAST = 3.06

Figure 42. A map depicting the location of the predictor points for storm surge at Boston and a calculation form.

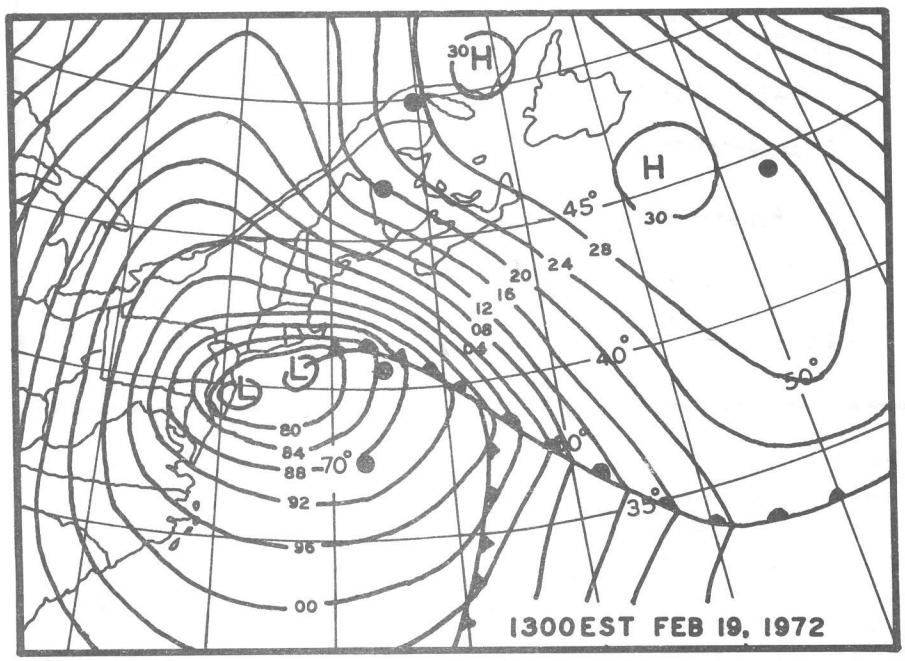

Figure 43. The sea-level pressure analysis for 1300 EST February 19, 1972. The dots indicate the location of the predictor points for Boston.

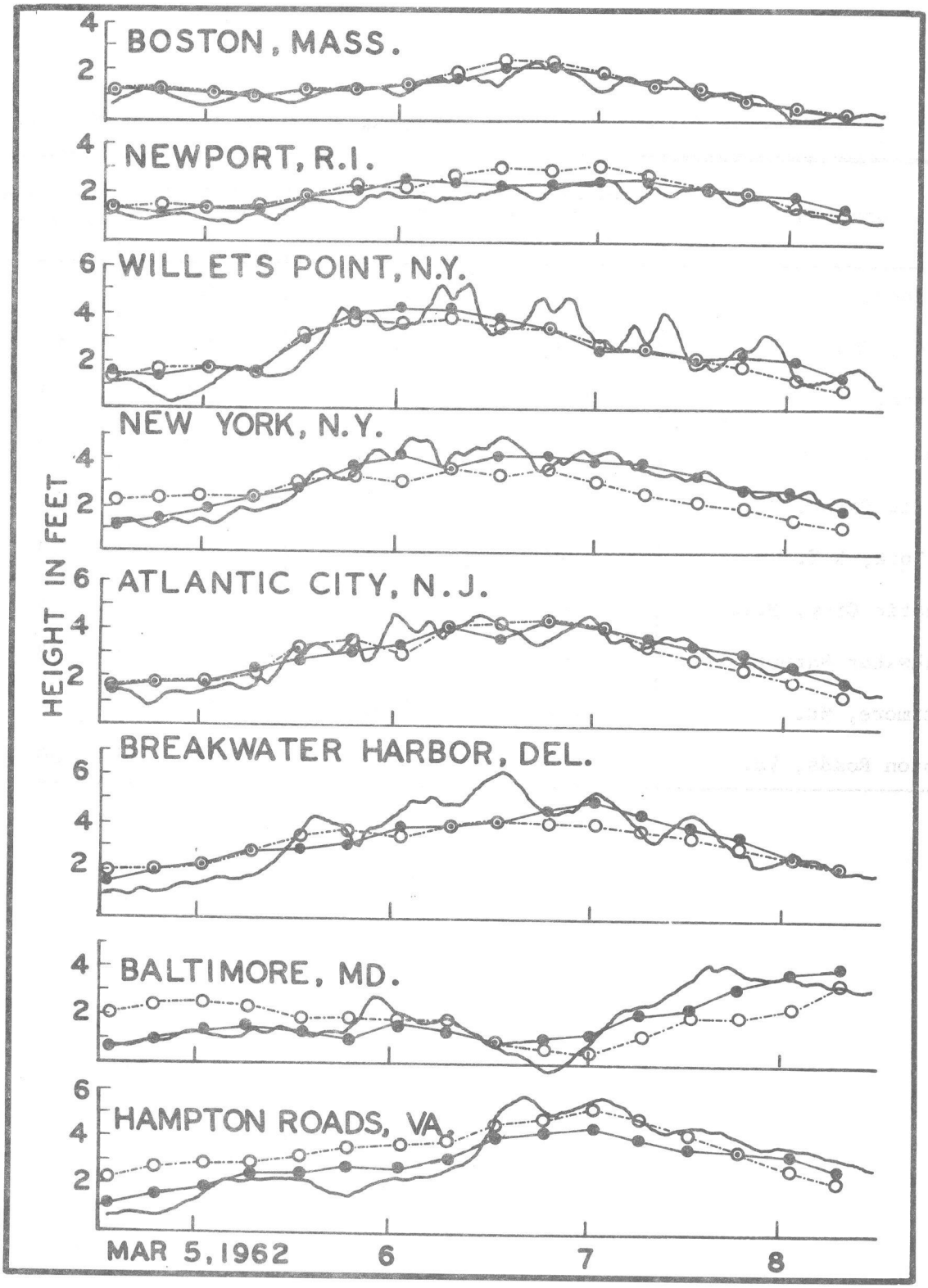

Figure 44. The calculated surge based on the sea-level pressure analysis for the automated and the manual methods and the observed surge for March 5 thru 8, 1962. The line connecting the dots is the automated method surge. The broken line and open circles is the manual method surge. The solid line is the observed surge.

Table 1.--Statistics for automated and manual storm surge forecast equations

Station	Correlation Coefficient		Number of sets of data	Number of storms
	Automated equations	Manual equations		
Portland, Me.	0.85	0.82	355	36
Boston, Mass.	0.84	0.82	502	48
Newport, R.I.	0.80	0.73	579	52
Stamford, Conn.	0.80	0.80	57	8
Willets Point, N.Y.	0.85	0.77	387	48
New York, N.Y.	0.84	0.74	596	53
Atlantic City, N.J.	0.84	0.77	688	58
Breakwater Harbor, Del.	0.82	0.78	646	53
Baltimore, Md.	0.87	0.62	575	34
Hampton Roads, Va.	0.88	0.72	455	30

Table 2.--Wind velocities recorded at some coastal locations during the storm of November 25-26, 1950

Nov. 1950	Portland Me.	Boston Mass.	Willets Point N.Y.	New York N.Y.	Atlantic City N.J.	Baltimore Md.	Hampton Roads Va.
24/01		NE/14 mph	N/12 mph	NE/10 mph		E/14 mph	SE/32 mph
07		NE/15	NE/15	E/7		E/8	ESE/37
13		NE/19	NE/19	E/13		ESE/25	SE/48
19		E/19	E/20	E/14		E/18	ESE/19
25/01		ESE/31	ENE/26	E/35		E/32	SSE/19
07		E/43	E/52	E/45		SE/22	SSE/6
13		E/41	SE/50	S/18		W/14	SSW/22
19		E/55	SSW/24	S/24		WSW/14	SW/20
26/01		SSW/12	SSW/16	S/24		S/10	SW/12
07		SW/9	SW/16	SE/10		S/18	S/8
13		S/10	SE/12	S/15		S/19	SSW/15
19		E/9	SW/12	W/12		S/9	SW/10
			Fastest mile				
Nov. 24	NE/20 mph	E/34 mph	-	E/23 mph	NE/20 mph	E/35 mph	SE/33 mph
Nov. 25	E/63	E/74	-	S/59	E/39	E/55	SE/37
Nov. 26	E/66	SE/80	-	S/33	E/72	SW/28	S/17

Table 3.--Wind velocities recorded at some coastal locations during the storm of November 5-8, 1953

Nov. 1953	Portland Me.	Boston Mass.	Willets Point N.Y.	New York N.Y.	Atlantic City N.J.	Baltimore Md.	Hampton Roads Va.
06/01	N/10 mph	N/24 mph	NNE/22 mph	N/12 mph		NE/22 mph	NE/18 mph
07	N/11	N/18	NE/28	NE/18		NE/23	NNE/24
13	NNE/13	NE/29	NE/36	NE/35		NNE/22	NNE/26
19	NNE/18	NE/39	NE/42	NE/30		NNE/23	N/24
07/01	NNE/21	NE/53	NE/46	NE/27		NNW/30	NNW/20
07	NNE/30	ENE/49	E/23	SW/26		WNW/20	NW/18
13	ENE/32	SE/11	SSW/18	SW/17		W/25	WNW/14
19	SSE/10	SSW/12	SSW/16	S/16		SW/16	W/6
			Fastest mile				
Nov. 06	NE/25 mph	NE/49 mph		NE/35 mph	NE/69 mph	NW/32 mph	NE/30 mph
Nov. 07	E/41	NE/67		SW/36	NE/68	NW/36	NW/24

Table 4.--Wind velocities recorded at some coastal locations during the storm of March 8-9, 1957

March 1957	Portland Me.	Boston Mass.	Willets Point N.Y.	New York N.Y.	Atlantic City N.J.	Baltimore Md.	Hampton Roads Va.
08/01	NNE/8 kt	NNE/11 kt	NE/15 kt	NE/11 kt		NE/16 kt	ENE/12 kt
04	NNE/9	NNE/12	ENE/16			ENE/14	N/3
07	N/9	NNE/16	ENE/20	NE/13		ENE/19	E/12
10	NE/18	NE/23	ENE/17			ENE/20	ESE/9
13	ENE/14	NE/24	ENE/15	NE/15		NE/16	S/8
16	NE/14	NNE/20	NE/22			ENE/14	NNW/9
19	NNE/16	NNE/26	NNE/17	NE/14		WNW/10	W/15
22	NNE/18	NE/31	NNE/20			WNW/18	WNW/16
09/01	NNE/25	NNE/31	N/11	NW/16		WNW/16	W/18
04	NNE/22	NNW/25	W/6			WNW/11	W/20
07	NE/18	W/16	WNW/10	W/21		W/18	WSW/18
10	SSE/23	SW/12	WSW/12			WNW/20	WNW/17
13	SSE/13	SW/14	WSW/20	W/31		WNW/24	W/20
16	SE/12	W/20	N/15	W/34		NW/30	NW/16
19	CALM	WSW/30	W/20	W/37		NW/12	NW/18
22	WSW/13	WSW/18	WNW/20	W/38		WNW/15	NW/18
			Fastest mile				
Mar. 08	NE/27mph	NE/45 mph		NE/18 mph	N/36 mph		W/34 mph
Mar. 09	SE/29	NE/45		W/38	W/32		NW/37

Table 5.--Wind velocities recorded at some coastal locations during the storm of March 5-8, 1962

March 1962	Boston Mass.	Willets Point N.Y.	New York N.Y.	Atlantic City N.J.	Baltimore Md.	Hampton Roads Va.
06/01	ENE/24 kt	NE/29 kt		E/25 kt	NNE/17 kt	SW/17 kt
04	ENE/28	ENE/30	NE/34 kt	E/30	NNE/19	SW/18
07	E/30	NE/36	NE/32	E/27	NE/19	SSW/12
10	ENE/33	NE/33	NE/32	E/30	ENE/20	SSW/9
13	ENE/34	NE/33	NE/34	ESE/25	NE/18	SW/7
16	ENE/32	NE/26	NE/32	E/30	N/16	NNW/12
19	ENE/31	NE/30	NE/38	E/30	NNE/20	N/20
22	ENE/30	NE/30	NE/48	E/30	NNE/15	N/22
07/01	ENE/32	NE/32	NE/35	ENE/26	N/15	NNE/28
04	ENE/34	NNE/32	NE/40	ENE/24	N/15	NNE/28
07	NE/30	NNE/30	NE/34	ENE/20	N/15	NNE/30
10	NE/25	NE/31	NE/40	ENE/20	NNE/17	NNE/25
13	NE/26	NE/30	NE/40	NNE/20	NNE/19	N/24
16	ENE/28	NE/21	NE/35	ENE/28	NNE/17	NNE/22
19	NE/18	NE/17	NE/30	NE/10	NE/11	NNE/22
22	NE/20	NE/18		NW/5	N/8	NNE/20
08/01	ENE/20	NNE/16	NE/18	NE/7	N/10	N/18
04	NE/17	NNE/17		N/6	NNW/8	N/17
07	NNE/18	N/18	NE/16	NNW/6	NE/8	NNE/17
10	NNE/15	NE/20		E/8	NE/8	NNE/15
13	E/9	ENE/10	NE/12	ESE/10	ESE/6	N/16
16	E/9	ENE/9		ESE/9	E/7	N/13
19	SE/5	E/8	E/9	ESE/4	E/5	NE/12
22	SW/4	S/9		CALM	SE/7	NE/11
			Fastest mile			
Mar. 06	NE/45 mph		NE/51 mph	NE/44 mph		NE/26 mph
Mar. 07	NE/47		NE/42	N/30		NE/41
Mar. 08	NE/28		NE/22	NNE/16		N/22

Table 6.--Wind velocities recorded at some coastal locations during the storm of January 23-24, 1966

Jan. 1966	Portland Me.	Boston Mass.	Willets Point N.Y.	New York N.Y.	Atlantic City N.J.	Baltimore Md.	Hampton Roads Va.
22/01	35/5 kt	31/06 kt	06/03 kt	36/04 kt	31/05 kt	28/03 kt	04/06 kt
04	36/6	31/07	04/07	36/05	36/03	32/02	04/14
07	34/5	35/05	05/08	36/05	02/04	06/05	04/16
10	34/5	36/05	06/08	09/08	08/06	05/07	07/12
13	07/6	09/09	05/11	09/06	09/12	06/04	08/14
16	16/4	08/07	05/13	09/09	08/14	08/10	09/15
19	CALM	04/06	08/10	05/10	11/15	07/13	07/21
22	36/5	08/15	08/11	05/11	10/22	08/15	08/17
23/01	04/5	08/16	07/17	05/16	09/27	07/17	09/14
04	04/11	09/17	08/17	05/16	08/32	06/08	24/18
07	06/14	10/24	08/21	05/21	08/27	32/13	25/22
10	09/23	09/30	08/17	36/19	17/15	33/15	25/20
13	09/20	08/30	07/23	36/23	28/28	29/19	28/20
16	06/24	07/27	04/23	36/21	30/32	29/20	27/15
19	06/18	05/23	34/14	32/09	30/26	28/14	27/17
22	06/20	03/18	34/15	29/32	31/26	31/20	28/17
				Fastest mile			
Jan. 22	N/8 mph	E/18 mph	NE/20 mph	NE/22 mph	09/29 mph	E/27 mph	E/36 mph
Jan. 23	E/29	E/43	NE/40	N/39	30/37	NW/30	NW/35

Table 7.--Wind velocities recorded at some coastal locations during the storm of November 10-13, 1968

Nov. 1968	Portland Me.	Boston Mass.	Willets Point N.Y.	New York N.Y.	Atlantic City N.J.	Baltimore Md.	Hampton Roads Va.
10/01	03/6 kt	01/6 kt	09/9 kt	09/7 kt	36/7 kt	35/7 kt	02/18 kt
04	01/7	01/5	08/13	05/12	03/11	02/9	02/28
07	04/9	01/10	06/17	05/14	04/17	36/12	36/27
10	04/10	07/14	05/18	05/17	04/16	33/13	33/15
13	02/12	06/27	02/15	36/15	35/16	34/16	30/12
16	02/10	36/25	36/20	36/12	31/16	33/13	33/9
19	03/18	01/28	33/15	32/10	31/11	32/10	30/13
22	35/12	35/20	35/13	27/6	32/8	32/10	28/8
11/01	36/13	34/12	01/12	36/6	31/8	28/7	30/8
04	33/6	34/11	01/11	36/7	31/7	27/5	31/6
07	31/9	32/8	02/5	36/3	34/6	28/7	27/6
10	32/13	32/11	04/7	36/6	01/4	36/9	35/7
13	30/10	32/10	04/7	36/4	05/6	22/3	02/8
16	34/8	34/12	02/9	36/9	07/8	06/5	07/8
19	36/5	35/10	03/9	36/9	05/9	05/9	04/14
22	02/5	02/9	07/15	05/13	07/14	05/10	05/20
12/01	CALM	06/16	06/20	05/15	06/16	06/23	06/23
04	02/5	06/12	06/27	05/19	06/30	03/24	18/10
07	03/8	08/20	06/43	05/27	07/32	36/14	18/16
10	02/12	08/34	07/25	05/30	07/16	36/20	24/22
13	05/15	08/31	05/27	05/22	17/16	31/15	26/30
16	06/12	07/29	04/20	36/15	27/3	31/19	27/20
19	03/15	10/13	01/12	36/12	30/18	31/20	28/16
22	04/15	13/11	33/14	32/14	27/14	28/20	29/16
13/01	36/9	14/15	29/15	27/10	27/17	28/16	27/16
04	12/9	19/14	30/17	27/14	28/19	29/15	27/12
07	15/7	26/16	29/17	27/14	27/21	29/15	26/9
10	36/7	27/17	29/20	27/15	28/21	31/20	26/17
13	32/8	28/22	30/21	27/15	30/22	32/20	30/15
16	31/12	29/22	31/28	32/15	28/20	30/12	29/12
19	32/8	30/24	31/23	27/16	28/19	28/18	29/13
22	32/12	30/24	31/23	32/15	29/15	28/13	30/08
			Fastest mile				
Nov.10	N/24 mph	N/40 mph	N/32 mph	NE/26 mph	32/22 mph	NW/19 mph	N/34 mph
Nov.11	N/19	NW/19	E/31	NE/23	07/18	NE/16	NE/40
Nov.12	NE/22	NE/54	NE/67	NE/51	06/39	N/35	NE/47
Nov.13	W/22	NW/30	NW/37	NW/29	28/29	NW/33	W/29

Table 8.--Fastest observed 1-minute wind speeds and directions for February 19 and 20, 1972. Data from the Environmental Data Service Publication, Local Climatological Data.

Location	Date	Direction	Speed (mph)
Boston, Mass.	Feb. 19	Northeast	47
	Feb. 20	Northwest	47
Portland, Me.	Feb. 19	East	37
	Feb. 20	North	37
Providence, R.I.	Feb. 19	Northeast	32
	Feb. 20	North-northwest	32
Bridgeport, Conn.	Feb. 19	Northeast	46
	Feb. 20	West-northwest	48
New York, N.Y. (La Guardia AP)	Feb. 19	Northeast	49
	Feb. 20	Northwest	37
Atlantic City, N.J.	Feb. 19	Northeast	40
	Feb. 20	West-northwest	40
Baltimore, Md.	Feb. 19	Northwest	38
	Feb. 20	Northwest	36
Norfolk, Va.	Feb. 19	West	40
	Feb. 20	West	37

Table 9. Values for manual storm surge calculation at Boston. Locations of points A through E are shown in figure 42.

$$SS(BOS) = 39.70 + .00187\,P(A)_t + .02444\,P(B)_t$$
$$-.08432\,P(D)_t - .01065\,P(E)_t + .02991\,P(C)_t$$

SEA-LEVEL PRESSURE IN MB	A'	B'	C'	D'	E'
950	41.48	23.22	28.41	-80.10	-10.12
952	41.48	23.27	28.47	-80.27	-10.14
954	41.48	23.32	28.53	-80.44	-10.16
956	41.49	23.36	28.59	-80.61	-10.18
958	41.49	23.41	28.65	-80.78	-10.20
960	41.50	23.46	28.71	-80.95	-10.22
962	41.50	23.51	28.77	-81.12	-10.25
964	41.50	23.56	28.83	-81.28	-10.27
966	41.51	23.61	28.89	-81.45	-10.29
968	41.51	23.66	28.95	-81.62	-10.31
970	41.51	23.71	29.01	-81.79	-10.33
972	41.52	23.76	29.07	-81.96	-10.35
974	41.52	23.80	29.13	-82.13	-10.37
976	41.53	23.85	29.19	-82.30	-10.39
978	41.53	23.90	29.25	-82.46	-10.42
980	41.53	23.95	29.31	-82.63	-10.44
982	41.54	24.00	29.37	-82.80	-10.46
984	41.54	24.05	29.43	-82.97	-10.48
986	41.54	24.10	29.49	-83.14	-10.50
988	41.55	24.15	29.55	-83.31	-10.52
990	41.55	24.20	29.61	-83.48	-10.54
992	41.56	24.24	29.67	-83.65	-10.56
994	41.56	24.29	29.73	-83.81	-10.59
996	41.56	24.34	29.79	-83.98	-10.61
998	41.57	24.39	29.85	-84.15	-10.63
1000	41.57	24.44	29.91	-84.32	-10.65
1002	41.57	24.49	29.97	-84.49	-10.67
1004	41.58	24.54	30.03	-84.66	-10.69
1006	41.58	24.59	30.09	-84.83	-10.71
1008	41.58	24.64	30.15	-84.99	-10.74
1010	41.59	24.68	30.21	-85.16	-10.76
1012	41.59	24.73	30.27	-85.33	-10.78
1014	41.60	24.78	30.33	-85.50	-10.80
1016	41.60	24.83	30.39	-85.67	-10.82
1018	41.60	24.88	30.45	-85.84	-10.84
1020	41.61	24.93	30.51	-86.01	-10.86
1022	41.61	24.98	30.57	-86.18	-10.88
1024	41.61	25.03	30.63	-86.34	-10.91
1026	41.62	25.08	30.69	-86.51	-10.93
1028	41.62	25.12	30.75	-86.68	-10.95
1030	41.63	25.17	30.81	-86.85	-10.97
1032	41.63	25.22	30.87	-87.02	-10.99
1034	41.63	25.27	30.93	-87.19	-11.01
1036	41.64	25.32	30.99	-87.36	-11.03
1038	41.64	25.37	31.05	-87.52	-11.05
1040	41.64	25.42	31.11	-87.69	-11.08
1042	41.65	25.47	31.17	-87.86	-11.10
1044	41.65	25.52	31.23	-88.03	-11.12
1046	41.66	25.56	31.29	-88.20	-11.14
1048	41.66	25.61	31.35	-88.37	-11.16

APPENDIX A

REGRESSION EQUATIONS FOR AUTOMATED STORM SURGE FORECAST METHOD

$$SS(PWM) = 32.40 - .05232\ P(33)_t + .00126\ P(13)_t - .03001\ P(22)_t - .06813\ P(24)_t + .07567\ P(18)_t + .02346\ P(40)_t + .01871\ P(16)_t$$

$$SS(BOS) = 48.31 + .01115\ P(41)_t + .01382\ P(12)_t - .03098\ P(33)_t - .00875\ P(16)_t + .04640\ P(18)_t - .04349\ P(32)_t - .03541\ P(34)_t$$

$$SS(NWP) = 29.33 - .00937\ P(40)_t + .02061\ P(11)_{t-12} - .02126\ P(42)_t - .03972\ P(39)_{t-6} + .05666\ P(25)_{t-6} - .03474\ P(34)_{t-12} - .02901\ P(32)_t + .02872\ P(48)_t$$

$$SS(SFD) = 24.06 + .06265\ P(12)_t - .07930\ P(31)_t - .03170\ P(40)_t + .05521\ P(18)_t - .02926\ P(27)_t$$

$$SS(LGA) = 24.11 - .09150\ P(40)_t - .02667\ P(17)_{t-6} - .09887\ P(39)_{t-6} - .02987\ P(27)_{t-12} + .08436\ P(48)_t + .14425\ P(24)_{t-6} - .03526\ P(50)_{t-6} + .03023\ P(7)_{t-6}$$

$$SS(NYC) = 24.29 - .00071\,P(47)_{t-6} + .02546\,P(17)_{t-6} - .05385\,P(42)_{t-6} - .03172\,P(30)_{t-6} + .05347\,P(24)_{t-6} - .09671\,P(39)_{t-6} + .05530\,P(32)_{t-6} + .02568\,P(45)_{t}$$

$$SS(ACY) = 37.35 + .03905\,P(48)_{t} + .02658\,P(17)_{t-12} - .04349\,P(42)_{t-12} + .04801\,P(24)_{t-6} - .08836\,P(40)_{t} - .05560\,P(47)_{t-6} + .03776\,P(32)_{t}$$

$$SS(BWH) = 55.93 - .01113\,P(48)_{t} + .09477\,P(24)_{t-6} - .01890\,P(41)_{t-6} - .07897\,P(47)_{t-6} - .04897\,P(42)_{t-12}$$

$$SS(BAL) = 76.17 - .02070\,P(30)_{t} + .00157\,P(33)_{t} + .04298\,P(12)_{t-36} - .05398\,P(48)_{t-36} + .05536\,P(32)_{t-24} - .02245\,P(30)_{t-12} + .03543\,P(40)_{t-6} - .03703\,P(43)_{t} - .06737\,P(45)_{t-12} - .01675\,P(41)_{t-30} - .01623\,P(1)_{t} - .01557\,P(28)_{t-36} + .05429\,P(40)_{t} + .05780\,P(32)_{t-12} - .07132\,P(31)_{t-6}$$

$$SS(ORF) = 59.68 - .02630\,P(17)_{t-18} - .03764\,P(55)_{t-6} - .04543\,P(50)_{t-24} + .09306\,P(31)_{t-6} - .06989\,P(46)_{t-24} + .06303\,P(24)_{t-24} - .05104\,P(47)_{t} + .01617\,P(12)_{t-24}$$

Where SS(STA) is the storm surge in tenths of feet, at forecast location (STA) at time t. P is the sea-level pressure in millibars at the indicated grid point. The subscript of pressure is the time in hours.

APPENDIX B

REGRESSION EQUATIONS FOR MANUAL STORM SURGE FORECAST METHOD

$$SS(PWM) = 50.92 - .04600\ P(33)_t + .01840\ P(13)_t - .01754\ P(22)_t - .04792\ P(24)_t + .04332\ P(18)_t$$

$$SS(BOS) = 39.70 + .00187\ P(41)_t + .02444\ P(12)_t - .08432\ P(33)_t - .01065\ P(16)_t + .02991\ P(18)_t$$

$$SS(NWP) = 52.07 + .00510\ P(40)_t + .00774\ P(12)_t - .05196\ P(42)_t - .04840\ P(31)_t + .03715\ P(18)_t$$

$$SS(SFD) = 24.06 + .06265\ P(12)_t - .07930\ P(31)_t - .03170\ P(40)_t + .05521\ P(18)_t - .02926\ P(27)_t$$

$$SS(LGA) = 14.69 - .10606\ P(40)_t + .12934\ P(17)_t + .09499\ P(48)_t - .08270\ P(31)_t - .04952\ P(50)_t$$

$$SS(NYC) = 20.04 + .01874\ P(48)_t + .09642\ P(18)_t - .06756\ P(40)_t - .03833\ P(27)_t - .02799\ P(31)_t$$

$$SS(ACY) = 34.62 + .00703\ P(48)_t + .00470\ P(17)_t - .08621\ P(40)_t - .03140\ P(42)_t + .07275\ P(24)_t$$

$$SS(BWH) = 51.13 - .02877\ P(48)_t + .00794\ P(17)_t - .05435\ P(42)_t - .05800\ P(39)_t + .08368\ P(24)_t$$

$$SS(BAL) = 53.36 - .05766\ P(30)_t + .13400\ P(33)_t - .06626\ P(43)_t - .12611\ P(31)_t + .06561\ P(39)_t$$

$$SS(ORF) = 31.27 - .02857\ P(17)_t - .07878\ P(56)_t + .10607\ P(24)_t - .04443\ P(42)_t + .01607\ P(9)_t$$

Where SS(STA) is the storm surge in tenths of feet, at forecast location (STA) at time t. P is the sea-level pressure in millibars at the indicated grid point.

(Continued from inside front cover)

WBTM TDL 25 Charts Giving Station Precipitation in the Plateau States From 850- and 500-Millibar Lows During Winter. August F. Korte, Donald L. Jorgensen, and William H. Klein, September 1969. (PB-187-476)

WBTM TDL 26 Computer Forecasts of Maximum and Minimum Surface Temperatures. William H. Klein, Frank Lewis, and George P. Casely, October 1969. (PB-189-105)

WBTM TDL 27 An Operational Method for Objectively Forecasting Probability of Precipitation. Harry R. Glahn and Dale A. Lowry, October 1969. (PB-188-660)

WBTM TDL 28 Techniques for Forecasting Low Water Occurrences at Baltimore and Norfolk. James M. McClelland, March 1970. (PB-191-744)

WBTM TDL 29 A Method for Predicting Surface Winds. Harry L. Glahn, March 1970. (PB-191-745)

WBTM TDL 30 Summary of Selected Reference Material on the Oceanographic Phenomena of Tides, Storm Surges, Waves, and Breakers. N. Arthur Pore, May 1970. (PB-192-449)

WBTM TDL 31 Persistence of Precipitation at 108 Cities in the Conterminous United States. Donald L. Jorgensen and William H. Klein, May 1970. (PB-193-599)

WBTM TDL 32 Computer-Produced Worded Forecasts. Harry R. Glahn, June 1970. (PB-194-262)

WBTM TDL 33 Calculation of Precipitable Water. L. P. Harrison, June 1970. (PB-193-600)

WBTM TDL 34 An Objective Method for Forecasting Winds Over Lake Erie and Lake Ontario. Celso S. Barrientos, August 1970. (PB-194-586)

WBTM TDL 35 Probabilistic Prediction in Meteorology: a Bibliography. Allan H. Murphy and Roger A. Allen, June 1970. (PB-194-415)

WBTM TDL 36 Current High Altitude Observations--Investigation and Possible Improvement. M. A. Alaka and R. C. Elvander, July 1970. (COM-71-00003)

NOAA Technical Memoranda

NWS TDL-37 Prediction of Surface Dew Point Temperatures. R. C. Elvander, February 1971. (COM-71-00253)

NWS TDL-38 Objectively Computed Surface Diagnostic Fields. Robert J. Bermowitz, February 1971. (COM-71-00301)

NWS TDS-39 Computer Prediction of Precipitation Probability for 108 Cities in the United States. William H. Klein, February 1971. (COM-71-00249)

NWS TDL-40 Wave Climatology for the Great Lakes. N. A. Pore, J. M. McClelland, C. S. Barrientos, and W. E. Kennedy, February 1971. (COM-71-00368)

NWS TDL-41 Twice-Daily Mean Monthly Heights in the Troposphere Over North America and Vicinity. August F. Korte, June 1971. (COM-71-00826)

NWS TDL-42 Some Experiments With a Fine-Mesh 500-Millibar Barotropic Model. Robert J. Bermowitz, August 1971. (COM-71-00958)

NWS TDL-43 Air-Sea Energy Exchange in Lagrangian Temperature and Dew Point Forecasts. Robert M. Reap, October 1971. (COM-71-01112)

NWS TDL-44 Use of Surface Observations in Boundary-Layer Analysis. H. Michael Mogil and William D. Bonner, March 1972. (COM-72-10641)

NWS TDL-45 The Use of Model Output Statistics (MOS) To Estimate Daily Maximum Temperatures. John R. Annett, Harry R. Glahn, and Dale A. Lowry, March 1972. (COM-72-10753)

NWS TDL-46 SPLASH (Special Program To List Amplitudes of Surges From Hurricanes) I. Landfall Storms. Chester P. Jelesnianski, April 1972. (COM-72-10807)

NWS TDL-47 Mean Diurnal and Monthly Height Changes in the Troposphere Over North America and Vicinity. August F. Korte and DeVer Colson, August 1972. (COM-72-11132)

NWS TDL-48 Synoptic Climatological Studies of Precipitation in the Plateau States From 850-, 700-, and 500-Millibar Lows During Spring. August F. Korte, Donald L. Jorgensen, and William H. Klein, August 1972. (COM-73-10069)

NWS TDL-49 Synoptic Climatological Studies of Precipitation in the Plateau States From 850-Millibar Lows During Fall. August F. Korte and DeVer Colson, August 1972.